Title: Conserved auxin signalling synergism through the canonical and ETT-mediated pathways promotes gynoecium development in members of the *Brassicaceae*

Running title: Auxin regulates gynoecium development

Heather Marie McLaughlin*[1,2], Tian-Feng Lü*[3,4], Bhavani Natarajan[1], Lars Østergaard[1,6], Yang Dong[1,3,4,5]

*Joint first authors

1- Department of Crop Genetics, The John Innes Centre, Norwich Research Park, Colney Lane, Norwich, NR4 7UH, UK. 2- Sainsbury Laboratory at Cambridge University, 47 Bateman Street, Cambridge, CB2 1LR, UK. 3-State Key Laboratory of Plant Diversity and Specialty Crops, Institute of Botany, Chinese Academy of Sciences, 20 Nanxincun, Xiangshan, Beijing 100093, China. 4- China National Botanical Garden, Beijing 100093, China. 5- University of Chinese Academy of Sciences, Beijing 100049, China. 6- Department of Biology, University of Oxford, South Parks Road, Oxford, OX1 3RB, UK

Corresponding**:** yang.dong@ibcas.ac.cn and heather.mclaughlin@slcu.cam.ac.uk

Keywords: Gynoecium, fruit, auxin, polarity, morphogenesis, signalling.

ORCIDs

Yang Dong: 0000-0003-2117-538X

Heather M. McLaughlin: 0000-0002-3020-7964

Bhavani Natarajan: 0000-0001-6852-7130

Tian-Feng Lü: 0000-0003-3110-1405

Lars Østergaard: 0000-0002-8497-7657

Summary Statement: Here the relationship between canonical and ETT-mediated auxin signalling machineries is investigated in *Arabidopsis* and *Capsella* revealing conserved synergism between these two pathways in *Brassicaceae* with distinct fruit shapes.

Abstract

Gynoecium polarity establishment is regulated by auxin, a phytohormone whose signal is transduced through several pathways. The relationship between the ETT and canonical TIR1/AFB pathways, and their relevance for carpel development beyond *Arabidopsis thaliana*, have not been investigated. The data presented here show that the expression patterns of canonical and ETT-mediated signalling components, and phenotypes of higher order mutants are shared between *Arabidopsis* and *Capsella rubella*. *tir1 afb2 ett* mutants partially phenocopy *ett arf4* double mutants, suggesting a role for AUXIN RESPONSE FACTOR 4 (ARF4) in the integration of canonical and ETT-mediated signalling. Comparative transcriptomics revealed that the auxin-independent mis-regulation of *YABBY* genes correlate with patterning defects observed in *Arabidopsis ett arf4* mutants. Together, the data presented suggest conserved synergism between canonical and ETT-mediated pathways in gynoecium polarity establishment in the *Brassicaceae*. Finally, the data suggest that ETT/ARF4 function to prevent the auxin-induced expression of a range of targets in *Arabidopsis*, consistent with activator-repressor ARF antagonism, and implying that the maintenance of auxin insensitivity by repressive ARFs is important for a range of biological processes.

Introduction

The gynoecium is the female reproductive organ produced in flowering plants which develops into the fruit. The gynoecium is produced in the inner-most whorl of the flower and is composed of several specialized tissues (Sessions and Zambryski, 1995). The gynoecium can be subdivided into three distinct regions along the apical-basal axis; the stigma, style; and ovary. The ovary is made up of two valves, which are separated from one another by the valve margins and medial replum. Gynoecium patterning and morphogenesis is dependent on the dynamic distribution of the phytohormone auxin (Moubayidin and Østergaard, 2014).

Auxin signalling occurs via several distinct pathways in *Arabidopsis* (Dharmasiri et al., 2005; Kepinski and Leyser, 2005; Simonini et al., 2016; Fendrych et al., 2018; Cao et al., 2019; Kuhn et al., 2020; Friml et al., 2022). The canonical auxin signalling pathway induces the expression of auxin sensitive genes in the nucleus (Paponov et al., 2008a), and is composed of three main components: Auxin/Indole-3-Acetic Acid repressor proteins (AUX/IAAs), Transport Inhibitor Response1/Arabidopsis F-box (TIR1/AFB) receptors, and Auxin Response Factors (ARFs). In the absence of auxin, ARFs are bound by AUX/IAAs, which recruit the TOPLESS (TPL) co-repressor, preventing the expression of auxin responsive genes (Szemenyei et al., 2008). Auxin increases the affinity of the TIR1/AFBs for AUX/IAAs. AUX/IAAs are subsequently degraded by the proteasome, allowing ARFs to promote auxin responsive gene expression (Dharmasiri et al., 2005; Kepinski and Leyser, 2005).

ARFs are classified into three distinct clades: A-ARFs, B-ARFs, and C-ARFs (Ulmasov et al., 1999; Tiwari et al., 2003; Finet et al., 2013). A-ARFs are transcriptional activators which readily interact with AUX/IAAs, whilst B and C ARFs are characterized as repressive, and interact with AUX/IAAs less readily (Ulmasov et al., 1999; Tiwari et al., 2003; Finet et al., 2013; Vernoux et al., 2011; reviewed in Guilfoyle & Hagen, 2012).

The ETTIN (ETT/ARF3)-mediated pathway was elucidated more recently in the context of its role in gynoecium development (Simonini et al., 2016; Kuhn et al., 2020). ETT is a B-class repressive ARF which lacks the C-terminal domain required for AUX/IAA interaction (Simonini et al., 2016), and functions independently of the canonical pathway (Kuhn et al., 2020). ETT recruits a TPL-HISTONE DEACETYLASE 19 (HDA19) complex to prevent the transcription of target loci in the absence of auxin. ETT interacts with auxin through its C-terminal ETTIN-SPECIFIC (ES) domain and undergoes a conformational change upon auxin binding which breaks the ETT-TPL-HDA19 complex. Histones then become acetylated, and genes are derepressed (Kuhn et al., 2020).

ett mutants exhibit gynoecium defects which phenocopy aberrations produced upon treatment with the auxin transport inhibitor N-1-Naphthylphthalamic Acid (NPA), highlighting the importance of ETT-mediated signalling for auxin related processes in carpel development (Nemhauser et al., 2000). Gynoecium morphogenesis is dependent on auxin in *Arabidopsis thaliana* (from here on, Arabidopsis; Moubayidin and Østergaard, 2014). However, studies on auxin signal transduction in the carpels have mainly focused on the role of the ETT-mediated pathway (Simonini et al., 2016; Simonini et al., 2017; Kuhn et al., 2020). An understanding of the relative contribution of canonical and ETT-mediated signalling to gynoecium development, and the relevance of this relationship outside of *Arabidopsis* has not been described.

Several canonical auxin receptors - *TIR1*, *AFB1*, *AFB2*, and *AFB3* - are expressed in the style of the developing gynoecium (Dharmasiri et al., 2005; Cecchetti et al., 2008). Higher order *tir1afb1245* mutants exhibit curled siliques and reduced fertility indicative of gynoecium defects (Prigge et al., 2020). AUX/IAA-interacting ARFs (Vernoux et al., 2011; Piya et al., 2014), are also involved in the regulation of gynoecium development (Nagpal et al., 2005; Wang et al., 2005; Pekker et al., 2005; Kelley et al., 2012), further supporting a role for the canonical pathway in this process.

ETT shares partial redundancy with its paralogous ARF, ARF4, which contains a C-terminal PB1-domain and is capable of AUX/IAA interaction (Pekker et al., 2005; Kelley et al., 2012; Finet et al., 2010; Vernoux et al., 2011). However, whilst the transcriptional targets of ETT in the gynoecium are well described (Simonini et al., 2017; Andres-Robin et al., 2020), those of ARF4 are not, and little is known about the roles of ETT and ARF4 in gynoecium development beyond *Arabidopsis*.

102 The *Brassicaceae* family display an impressive array of fruit shape diversity including for example
103 cylindrical, spherical, disc and heart-shaped fruits (Łangowski et al., 2016). Interestingly, gynoecia from
104 species producing highly divergent fruit shapes still maintain the same general organization of tissues
105 with two or more carpels and an apical radial style topped with stigmatic papillae (Langowski et al.,
106 2016). Members of the *Brassicaceae* family therefore provide excellent models to study conserved
107 mechanisms of carpel development. It was recently shown that gynoecium development in *Capsella*
108 *rubella* (from here on *Capsella*), which diverged from *Arabidopsis* around 8 million years ago, and
109 produces heart shaped fruits, is also dependent on auxin dynamics throughout development (Dong et
110 al., 2019). However, the relative contributions of the canonical and ETT-mediated pathway to signal
111 transduction in *Capsella* fruit development are not known.
112 Here, *tir1 afb2 ett* mutants were generated in *Arabidopsis and Capsella.* In both species, the triple
113 mutant showed exacerbation of the *ett* phenotype suggesting that the canonical and ETT-mediated
114 pathways function synergistically in gynoecium development, and that this is conserved within the
115 *Brassicaceae*. Furthermore, *the tir1 afb2 ett* triple mutant partially phenocopied the *ett arf4* double
116 mutant in both species, suggesting a role for ARF4 in the integration of signalling between the
117 canonical and ETT-mediated pathways. A comparative transcriptomics analysis was conducted to
118 identify distinct and overlapping ETT and ARF4 targets in *Arabidopsis*. The data presented suggest that
119 ETT and ARF4 regulate distinct and overlapping targets independently of auxin including YABBY
120 transcription factors (TFs), and the mis-regulation of these genes correlates with the phenotypes
121 observed in the *Arabidopsis* mutants.
122 Finally, auxin sensitive transcriptomics in *Arabidopsis* suggest that ETT and ARF4 maintain the auxin
123 insensitivity of a range of target loci, many which became upregulated in response to auxin upon their
124 mutation, suggesting that A-B ARF antagonism previously observed in *Marchantia* (Kato et al., 2020)
125 and *Physcomitrium* (Lavy et al., 2016) may regulate a range of biological processes in *Arabidopsis.*
126 Together, the findings presented reveal conserved synergism between the canonical and ETT-
127 mediated pathway machineries in *Arabidopsis* and *Capsella*, identify auxin independent targets of ETT
128 and ARF4 in *Arabidopsis*, and suggest that the maintenance of auxin insensitivity at target loci plays
129 an important role in the regulation of a range of responses to environmental stresses.
130
131 **Results**
132
133 **Canonical and ETT-mediated pathway components are co-expressed during gynoecium**
134 **development in *Arabidopsis* and *Capsella.***

135 To assess whether the canonical and ETT-mediated pathways may co-regulate processes during
136 *Arabidopsis* gynoecium, we first studied the expression of GUS reporter lines for *ETT*, *TIR1*, *AFB2* and
137 *AFB3* during gynoecium development (Fig. 1). In *Arabidopsis*, *ETT* is expressed throughout the valves
138 of the gynoecium, and is most highly expressed at the apex of the valves in the region which gives rise
139 to the style at stage 10-12 (Fig. 1). At later stages *ETT* expression is much lower in the valves and
140 becomes mainly restricted to the style and replum. *AtTIR1*, *AtAFB2* and *AtAFB3* are also expressed
141 throughout the valves during stage 10-11 of gynoecium development, like *AtETT* (Fig. 1). *AtTIR1*
142 expression becomes reduced in the valves after stage 13 of development and is restricted to the style
143 and replum at stage 14. *AtAFB2* is also restricted to the style from stage 13 of gynoecium development,
144 whilst *AtAFB3* expression remains strongest in the apical valves, stigma, and style at stage 12-13 (Fig.
145 1). *AtAFB3* is then restricted to the style and stigma from stage 14 of gynoecium development.
146 The expression of the canonical and ETT-mediated signalling machinery within the same domains
147 suggests that both pathways may be involved in gynoecium development, particularly in valve and
148 style development in *Arabidopsis*.
149 To assess whether a role for both pathways is conserved, similar reporter lines were generated to
150 assess the expression patterns of *ETT*, *TIR1*, *AFB2* and *AFB3* in *Capsella* (Fig. 2). *CrETT* is expressed
151 strongly in the apical tissues of the gynoecium and the ovules during stage 10*, whilst CrTIR1, CrAFB2,*
152 *and CrAFB3* are expressed ubiquitously across the gynoecium at this stage (Fig. 2). *CrETT* is then most
153 strongly expressed in the style from stage 11-14. *CrTIR1*, *CrAFB2* and *CrAFB3* are continually expressed
154 in the apical valves and style from stage 11-13, and at stage 14 their expression levels are highest in
155 the outgrowing shoulders of the *Capsella* fruit, although *CrTIR1* is expressed at lower levels than
156 *CrAFB2* and *CrAFB3* (Fig. 2).
157 Together, these data suggest shared roles for the canonical and ETT-mediated pathways in valve
158 and style development in both *Arabidopsis* and *Capsella* and suggest a role for the canonical pathway
159 in post fertilization valve outgrowth in *Capsella*, which may contribute to heart-shaped fruit formation.
160
161 **Phenotypic analyses suggest synergism between canonical and ETT-mediated pathways is**
162 **conserved in other members of the *Brassicaceae*.**
163 To understand the relationship between the canonical and ETT-mediated auxin signalling pathways
164 during gynoecium development, *tir1-1 afb2-3 ett-3* triple mutants were generated in *Arabidopsis*, and
165 the resulting phenotypes were assessed compared to single and double mutants (Fig. 3). ETT functions
166 partly redundantly with ARF4, which shares ETT's expression domain in the valves and apical tissues
167 of the gynoecium during development (Fig. S1). ARF4 interacts with the canonical pathway AUX/IAAs

168 (Vernoux et al., 2011), implicating it in the canonical pathway. The *arf4-2* single mutants and *ett-3*
169 *arf4-2* double mutants were therefore included in this analysis (Fig. 3).
170 The *ett-3* mutant (Fig. 3B,H,N) exhibited reduced valves, a loss of radial symmetry in the style, and
171 over-proliferation of stigmatic tissues at later developmental stages (Fig. 3H,N), whilst the *arf4*-2 (Fig.
172 3C,I,O) and *tir1-2 afb2-3* (Fig. 3D,J,P) mutants resembled wild type (Fig. 3A,G,M). The *ett-3* phenotype
173 (Fig. 3B,H,N) was exacerbated in both *ett-3 arf4-2* (Fig. 3E,K,Q) and *tir1-1 afb2-3 ett-3* (Fig. 3F,L,R).
174 Valves in *ett-3 arf4-2* gynoecia were significantly reduced, producing an open ovary with ectopic
175 ovules and few stigmatic papillae (Fig. 3E,K,Q). The *ett-3 arf4-2* gynoecia lacked a style and split into
176 two distinct lobes with stigmatic papillae at their tips (Fig. 3E,K,Q). Similarly, *tir1-1 afb2-3 ett-3*
177 mutants exhibited enhanced valve reduction relative to *ett-3* mutants, producing a partially open
178 ovary with ectopic ovules, and no discernable style or replum (Fig. 3F,L,R). The stigmatic papillae in
179 *tir1-1 afb2-3 ett-3* gynoecia also developed atop two lobes produced at the apex, and exhibited over
180 proliferation of stigmatic tissues at later developmental stages comparable to those observed in *ett-3*
181 (Fig. 3B,F,H,L,N,R).
182 The exacerbation of the *ett-3* phenotype by *tir1-1 afb2-3* mutation demonstrates that the canonical
183 and ETT-mediated pathways function synergistically to promote gynoecium development.
184 Furthermore, the phenotypic similarities between *ett-3 arf4-2* and *tir1-1 afb2-3 ett-3* mutants,
185 especially at the early stages of gynoecium development, suggest that ETT/ARF4 and TIR1/AFB2
186 regulate similar processes in gynoecium development, and further implicate ARF4 in the canonical
187 pathway.
188 To assess whether synergism between the canonical and ETT-mediated pathways is conserved in
189 other *Brassicaceae* species, the same mutant combinations were generated by CRISPR/Cas9 in
190 *Capsella* (Fig. 4). As in *Arabidopsis*, the *Capsella arf4* mutants (Fig. 4C,I,O) resembled wild type (Fig.
191 4A,G,M), whilst *Crett* displayed valve reduction, stigmatic over proliferation and breakage in the radial
192 symmetry of the style (Fig. 4B,H,N). Whereas the *Arabidopsis tir1-1 afb2-3* mutant phenocopied wild
193 type, valve reduction was observed in the *Crtir1afb2* mutant, and this persisted at later developmental
194 stages so that the shoulders of the heart never fully elongated (Fig. 4,D,J,P). This suggests a more
195 prominent role for the canonical pathway in valve outgrowth in *Capsella* than in *Arabidopsis* and
196 implicates the canonical pathway in heart-shaped fruit development.
197 In *Arabidopsis*, the *ett-3 arf4-2* mutant exhibited the strongest phenotypes, producing a completely
198 open ovary, whilst *the tir1-1 afb2-3 ett-3* mutants exhibited less severe valve reduction defects (Fig.
199 3). However, *Crettarf4* (Fig. 4E,K,Q) and *Crtir1afb2ett* (Fig. 4F,L,R) mutants exhibited phenotypes
200 which were similar in severity. Both lines produced open ovaries with ectopic ovules atop a
201 hyperextended stalk like structures (Fig. 4E,F,K,L,Q,R). As in *Arabidopsis*, stigmatic tissues formed at

202 the apex of structures at the lateral edges of the gynoecium (Fig. 4E,F,K,L). Taken together these data
203 suggest that the synergism between canonical and ETT-mediated pathways in gynoecium
204 development is conserved between *Arabidopsis* and *Capsella* and may therefore be broadly relevant
205 for gynoecium development across the *Brassicaceae* family.
206
207 **Comparative transcriptomics in *Arabidopsis* dissect distinct and overlapping targets of ETT and ARF4**
208 **in gynoecium development.**
209 ETT is known to function partially redundantly with ARF4 in the regulation of gynoecium development
210 (Pekker et al., 2005; Finet et al., 2010; Kelley et al., 2012). Whilst ETT-mediated signalling and the
211 regulation of ETT-target genes are relatively well studied in the gynoecium (Simonini et al., 2016;
212 Simonini et al., 2017; Kuhn et al., 2020), a global understanding of how ARF4 regulates its targets, and
213 which genes it modulates in conjunction with ETT, is lacking. The phenotypic similarities between *ett*
214 *arf4* and *tir1 afb2 ett* mutant gynoecia, along with the observation that ARF4 physically interacts with
215 AUX/IAAs (Vernoux et al., 2011), implicate ARF4 in the canonical pathway.
216 To better understand how ARF4 regulates its targets both alone and together with ETT, a
217 comparative transcriptomic analysis (RNA sequencing, from here on RNA-Seq) was conducted utilizing
218 whole inflorescence tissues of *Arabidopsis* Col-0, *ett-3, arf4-2, and ett-3 arf4-2* lines treated with 100
219 μM Indole-3-Acetic Acid (IAA) and 10 μM N-1-Naphthylphthalamic Acid (NPA) or mock treatments for
220 one hour.
221 A principal component analysis revealed that the lines differed more by genotype than by auxin
222 treatment (Fig. S2), and many genes which are reportedly auxin responsive (Paponov et al., 2008)
223 were modulated in response to auxin in wild type plants, indicating that the auxin treatment was
224 effective (Table S1). *PINOID*, a previously well-characterized ETT target (Simonini et al., 2016; Simonini
225 et al., 2017; Kuhn et al., 2019) which is upregulated in wild type in response to auxin (Kuhn et al., 2020)
226 was not identified as an auxin sensitive gene within this study. Previous transcriptomics analyses
227 aiming to identify ETT targets utilized different schedules of auxin treatment (Kuhn et al., 2020;
228 Simonini et al., 2017) which may explain the observed discrepancies. Significant overlap was however
229 observed between genes mis-regulated in *ett-3* mutants between this study and Simonini et al., 2017
230 (Fig. S3; Table S2 and S3). The data were analyzed to identify auxin independent ETT/ARF4 targets in
231 accordance with the schema in Fig. S4. Two datasets each consisting of three lists of genes were used
232 for this analysis. The first dataset comprised lists of genes which were differentially expressed relative
233 to wild type in *ett-3*, *arf4-2,* and *ett-3 arf4-2* after mock treatment, whilst the second dataset
234 comprised the same after IAA treatment. These lists were compared to generate two three-way Venn
235 diagrams, one for each dataset. The data were then compared across mock and auxin treatments to

236 identify genes which are mis-regulated in the same manner in both the presence and absence of auxin.
237 Any auxin sensitive genes within these lists were removed, leaving genes which are regulated by ETT
238 and ARF4 independently of auxin. Based on where these genes positioned within a three-way Venn
239 diagram, models of gene behavior were devised which may explain the observed patterns of statistical
240 significance (Fig. 5; Fig. S5).
241 Gene Ontology (GO) term analyses were conducted in Shiny GO (Version 0.77, Ge et al., 2020) to
242 identify biological processes which are enriched within each target category (Fig. 5) compared to a
243 background list composed of all genes expressed in the RNA-seq experiment (Supplemental data File
244 2).
245
246 **ETT and ARF4 redundantly regulate cell fate commitment independently of auxin in *Arabidopsis*.**
247 The transcriptomics analysis identified 98 genes (53 up, 45 down) which were significantly mis-
248 regulated in *ett-3 arf4-2* relative to wild type in accordance with their redundant regulation by ETT
249 and ARF4 independently of auxin (Fig. 5A,B; Fig S5). GO term analysis indicated significant enrichment
250 within this list for genes involved in cell fate commitment, (Table 1; Fig. 5), including *CLAVATA3/ESR-*
251 *RELATED 19* (*CLE19*), *NO TRANSMITTING TRACT* (*NTT*), and *FAMA*, which were significantly
252 upregulated; and *YABBY2* (*YAB2*) and *YAB5,* and *ATMYC1* which were significantly downregulated in
253 *ett-3 arf4-2* (Fig. 5C; Fig. 6; Table 1).
254
255 **Table 1: Genes which are significantly differentially expressed in *ett-3 arf4-2* mutants relative to**
256 **wild type both in the presence and absence of auxin, consistent with their redundant regulation by**
257 **ETT and ARF4, and whose mis-regulation correlates with phenotypes observed in this line**.

Locus	Name	Log2Fold vs WT mock in *ett-3 arf4-2* mock	Log2Fold vs WT IAA in *ett-3 arf4-2* IAA	Significant in all treatments	GO term
AT3G24225	*CLE19*	2.39	2.27	True	cell fate commitment
AT3G57670	*NTT*	1.01	1.22	True	cell fate commitment
AT2G26580	*YAB5*	-1.6	-1.7	True	cell fate commitment
AT3G24140	*FAMA*	1.66	1.57	True	cell fate commitment
AT1G08465	*YAB2*	-1.94	-2.04	True	cell fate commitment
AT4G00480	*ATMYC1*	-1.29	-1.46	True	cell fate commitment
AT1G70560	*TAA1*	1.61	1.34	True	Indole-acetic acid biosynthetic process

AT5G03790	*ATHB-51*	1.15	1.13	True	floral meristem determinacy
AT2G33880	*WOX9*	1.66	1.90	True	regulation of meristem growth
AT1G80080	*TMM*	-1.04	-1.09	True	stomatal complex formation

258

259 The YABBY transcription factors, *YAB2* and *YAB5*, which are implicated in abaxial cell fate
260 specification, were constitutively downregulated in the double mutant (Table 1; Fig. 6), and this
261 correlated with the abaxial defects overserved in the leaves (Fig. S6 A-C), and patterning defects
262 observed in the gynoecium of this line (Fig. 3).

263 *FAMA,* a regulator of guard cell differentiation in the stomatal lineage, was upregulated in *ett-3*
264 *arf4-2*, and *TOO MANY MOUTHS* (*TMM*), another stomatal regulator, was constitutively
265 downregulated (Table 1). Along with the mis-regulation of stomatal lineage genes in *ett-3 arf4-2*,
266 stomatal defects were also observed on the abaxial surface of *ett-3 arf4-2* leaves (Fig S6). Finger-like
267 protrusions, which resemble the midvein in wild type plants, were produced from the abaxial surface
268 of *ett-3 arf4-2* leaves (Fig. SB,C). In wild type, the midvein lacks stomata, but the projections in *ett-3*
269 *arf4-2* exhibited stomata across the surface of these structures (Fig. S6C).

270 The WUSCHEL related homeobox transcription factor *WOX9*, the CLAVATA3-related peptide
271 encoding gene *CLE19,* and the gene encoding HD-ZIP I transcription factor *ARABIDOPSIS THALIANA*
272 *HOMEOBOX 51* (*ATHB-51*), were constitutively upregulated in *ett-3 arf4-2* (Table 1); these genes are
273 implicated in meristematic regulation. The mis-regulation of these genes correlates with variability in
274 the numbers of floral organs produced within *ett-3 arf4-2* flowers (Fig. S6D-H), suggesting a role for
275 ETT and ARF4 in floral meristem regulation.

276 The auxin biosynthesis gene *TAA1*, which promotes the production of auxin through the IPA
277 pathway, was constitutively upregulated in the double mutant (Table 1), suggesting that auxin
278 biosynthesis is also regulated redundantly by ETT and ARF4 independently of auxin.

279 Together, these data correlate with phenotypes observed in the *ett-3 arf4-2* mutant and suggest
280 that ETT and ARF4 may redundantly regulate cell fate specification independently of auxin in a range
281 of biological contexts, including axis specification of lateral organs.

282

283 **Transcriptomics identify ETT and ARF4-specific targets in *Arabidopsis***

284 Transcriptomics revealed 76 targets which became similarly mis-regulated in both *ett-3* and *ett-3 arf4-*
285 *2*, consistent with their ETT-specific regulation (Fig. 5A,B; Fig. S5). The list of ETT-specific targets was

286 enriched in GO term analysis for genes involved in gynoecium development, carpel development,
287 floral whorl development, floral organ development, and cellular response to light intensity (Table 2;
288 Fig. 5C; Fig. 7). The list included zinc finger transcription factor *JAGGED* (*JAG*), the YABBY transcription
289 factor *CRABSCLAW* (*CRC*), and basic-Helix-Loop-Helix TF *INDEHISCENT (IND)* which have previously
290 been implicated in gynoecium development (Table 2; Fig. 7). *JAG* expression was constitutively
291 downregulated in *ett-3* and *ett-3 arf4-2* mutants relative to wild type independently of auxin. JAG
292 functions with NUBBIN (NUB) to regulate gynoecium development (Dinneny et al., 2006). As in *ett-3*
293 and *ett-3 arf4-2*, *jag nub* mutants show apical defects in the gynoecium and altered floral organ
294 development (Fig. 3; Fig. S6D-H). *CRC* was constitutively downregulated in *ett-3* and *ett-3 arf4-2*, and
295 the knockdown of this gene has previously been shown to cause apical gynoecium defects in
296 *Arabidopsis* (Bowman & Smyth, 1999). The mis-regulation of these genes therefore correlates with
297 phenotypes observed in the *ett-3* and *ett-3 arf4-2* mutant gynoecia.
298
299 **Table 2: Genes which are significantly differentially expressed in *ett-3* and *ett-3 arf4-2* mutants**
300 **relative to wild type both in the presence and absence of auxin, consistent with their ETT-specific**
301 **regulation**.

Locus	Name	Col-0 vs ett-3 mock log2fold change	Col-0 vs ett-3 IAA log2 fold change	Col-0 vs ett-3 arf4-2 mock log2fold change	Col-0 vs ett-3 arf4-2 IAA log2fold change	Significance In all groups	Go Terms
AT1G69180	*CRC*	-0.44	-0.42	-1.12	-1.02	True	Carpel Development
AT5G21150	*AGO9*	-1.87	-1.78	-0.82	-0.83	True	Floral organ development
AT4G09960	*STK*	-0.60	-0.68	1.27	1.21	True	Carpel Development
AT3G22840	*ELIP1*	1.63	1.75	1.41	1.35	True	Response to light intensity
AT1G29440	*SAUR63*	-1.18	-1.43	-1.08	-1.15	True	Floral organ development

AT1G68480	*JAG*	-0.96	-0.72	-2.97	-1.88	True	Carpel development
AT4G14690	*ELIP2*	1.54	1.13	1.56	1.14	True	Response to light intensity
AT4G00120	*IND*	-2.82	-1.38	-3.03	-3.61	True	N/A valve margin specification (Liljegren et al., 2004)

Transcriptomics revealed several groups of genes regulated by ETT and ARF4 which did not appear to regulate gynoecium development. This included 134 genes mis-regulated only in *ett-3* single mutants, nine genes mis-regulated only in *arf4-2* single mutants, and nine genes mis-regulated in both *ett-3* and *arf4-2* single mutants (Fig. 5A,B), which were not enriched in GO term analysis, and are not discussed further.

Whilst the *arf4-2* mutant appeared as wild type (Fig. 3), 49 ARF4-specific genes were identified (Fig. 5A,B; Fig. S5). This list was enriched for genes involved in the regulation of microtubule polymerization and related GO terms (Fig. 5C) and did not contain any known regulators of gynoecium development, suggesting that ARF4 mainly functions in conjunction with ETT to elicit its auxin-independent effects in the carpels.

151 genes were significantly mis-regulated in all mutants relative to wild type, consistent with their regulation by ETT/ARF4 heterodimers (Fig. 5A,B; Fig. S5). This list was significantly enriched in GO term analysis for genes involved in secondary metabolism including S-glycoside, glucosinolate and glycosinolate biosynthesis (Fig. 5C).

Together, the transcriptomics data suggest that ETT and ARF4 regulate distinct and overlapping targets independently of auxin to promote gynoecium development and imply that ARF4 mainly functions with ETT to promote its auxin independent effects on gynoecium development.

Auxin sensitive analysis in *Arabidopsis* suggests redundant maintenance of auxin insensitivity by ETT and ARF4

Gynoecium morphogenesis is dependent on the dynamic distribution of auxin (Moubayidin & Østergaard, 2014), and gynoecium defects of *ett-3 arf4-2* mutants suggest a role for ETT and ARF4 in the transduction of auxin signalling (Pekker et al., 2005). A second analysis was therefore conducted

326 in *Arabidopsis* to assess how the auxin response varies from wild type in the mutants. Genes which
327 were significantly auxin responsive in wild type were compared to genes which were significantly auxin
328 responsive in each mutant background (*ett-3*, *arf4-2,* and *ett-3 arf4-2*).
329 Few genes were identified in the auxin sensitive analysis with a known role in gynoecium
330 development. 179 genes were auxin sensitive only in the *ett-3 arf4-2* mutant background (44 up and
331 135 down upon auxin treatment, Fig. 8) consistent with their redundant regulation by ETT and ARF4,
332 which maintain their auxin insensitivity. This list was enriched for a range of GO terms including pectin
333 metabolism/catabolism (Fig. 9A). The mis-regulation of pectin methylesterification has previously
334 been linked to gynoecium defects in *ett* mutants (Andres-Robin et al., 2018), and several pectin
335 methlyesterases (PMEs) and pectin methylesterase inhibitors (PMEIs) have been previously identified
336 as direct ETT targets (Andres-Robin et al., 2020). The list of redundantly regulated ETT/ARF4 targets in
337 the auxin sensitive analysis conducted here included *PME23*, *PME28*, *PME48*, *PME49, and* members
338 of the pectin lyase superfamily (*AT1G05660, AT3G07850, AT5G48140, AT3G07830*, *AT3G07840,*
339 *AT3G14040*).
340 None of the other gene lists assessed in the auxin sensitive analysis contained known regulators of
341 gynoecium development, but the data did implicate ETT and ARF4 in the maintenance of auxin
342 insensitivity at target loci involved in a range of biological processes, which then become auxin
343 sensitive upon ETT/ARF4 mutation consistent with previously proposed models of A-B ARF
344 antagonism.
345
346 **Auxin sensitive analysis reveals patterns of gene regulation consistent with A-B ARF antagonism.**
347 Previous studies in *Marchantia polymorpha* and *Phiscomitrium patens* found antagonism between A-
348 and B-ARFs to regulate the auxin sensitivity of tissues (Kato et al., 2020; Lavy et al., 2016), with the
349 auxin response being promoted by A-ARFs and inhibited by B-ARFs. Within the auxin sensitive analysis
350 several groups of genes were identified which behave in a manner consistent with A-B ARF antagonism
351 (Fig. 8). Firstly, 44 genes (out of 179) became upregulated in response to auxin only in *ett-3 arf4-2*
352 mutants, suggesting that ETT and ARF4 act redundantly to prevent their auxin responsiveness (Fig. 8).
353 Secondly, a further 143 genes (out of 143) were auxin insensitive in wild type and upregulated in
354 response to auxin in all mutant backgrounds, suggesting that ETT-ARF4 dimers maintain auxin
355 insensitivity at these loci (Fig. 8). Interestingly, ETT and ARF4 showed physical interactions in Yeast 2-
356 Hybrid (Y2H) assays (Fig. S7). ETT-ARF4 interaction was dependent on the presence of the ARF4 DNA
357 binding domain and was not sensitive to auxin (Fig. S7). Together the Y2H and RNA seq data suggest
358 that ETT and ARF4 can form heterodimers to regulate gene expression.

359 Finally, 194 genes (out of 199) were auxin insensitive in wild type and became upregulated upon
360 auxin treatment in *arf4-2* and *ett-3 arf4-2* mutants, consistent with the ARF4-specific prevention of
361 their auxin sensitivity (Fig. 8). GO term analysis showed that list of 44 redundantly regulated genes
362 which become auxin responsive in *ett-3 arf4-2* mutants are involved in plant-pathogen interactions.
363 The list of heterodimer targets which became auxin responsive in all mutant backgrounds were
364 enriched for loci involved in responses to environmental stresses, including biotic stimuli and hypoxia
365 (Fig. 9). The list of ARF4-specific targets was also enriched for similar GO terms (Fig. 9). Together these
366 data suggest a role for ETT and ARF4 in the regulation of a range of responses to biotic and abiotic
367 stress. Consistent with the hypothesis that ETT and ARF4 may antagonise A-ARFs, *ARF5*, *ARF6,* and
368 *ARF8*, which are A-class activators, are expressed in the gynoecium at various stages of development
369 (Fig.S8), however future studies will be required to assess whether they share antagonistic roles to
370 ETT and ARF4 in the regulation of environmental stress.
371
372
373 **Discussion**
374
375 **Synergism between canonical and ETT-mediated signalling components in gynoecium development.**
376 The phenotypic and expression analyses presented here suggest the existence of synergistic
377 regulation between the canonical and ETT-mediated pathways in gynoecium development, and that
378 this mechanism is conserved between *Arabidopsis* and *Capsella*. Indeed, previous studies in both
379 *Arabidopsis* and *Capsella* have shown that the dynamic distribution of auxin plays an important role
380 in gynoecium development (Moubayidin and Østergaard, 2014; Dong et al., 2019).
381 Whilst a role for ETT in style development has been observed in *Brassica rapa* (Simonini et al.,
382 2018), ETT's role in *Capsella* fruit development had not been characterized prior to this study. In
383 *Arabidopsis* ETT was known to function partially redundantly with ARF4 in gynoecium development
384 (Pekker et al., 2005; Finet et al., 2010). Here, we show that as in *Arabidopsis*, ETT and ARF4 function
385 partially redundantly in *Capsella*; phenotypes present in *Crett* mutants are exacerbated in *Crett arf4*,
386 suggesting that ARF4 shares some, but not all, of its functionality with ETT.
387 Furthermore, the *tir1 afb2 ett* triple mutant phenocopies *ett arf4* mutants in both species studied,
388 suggesting a role for ARF4 in the integration of signalling with the canonical pathway. Consistent with
389 this hypothesis, ARF4 has previously been shown to interact with AUX/IAAs of the canonical pathway
390 through its C-terminal domain (Vernoux et al., 2011). Structural evolution studies have previously
391 indicated that ETT and ARF4 arose from the duplication of a non-truncated ARF prior to the radiation
392 of extant angiosperms (Finet et al., 2010), and that the truncation of either ETT or ARF4, so that they

393 lack the C-terminal PB1 domain, is common in the angiosperm lineage. However, whilst *Arabidopsis*
394 ETT was more able to rescue *ett* phenotypes when truncated, ARF4 required its C-terminal domain to
395 function (Finet et al., 2010), consistent with the idea that AUX/IAA interaction is required for ARF4
396 activity. However, the C-terminal PB1 domain has also been shown to facilitate ARF homodimer and
397 homo-oligomerization (Davis et al., 2020; Korasick et al., 2015), meaning that further studies will be
398 required to understand the mechanism of ARF4 action, and how it integrates the canonical and ETT-
399 mediated pathways.
400
401 **Comparative transcriptomics correlate with phenotypic defects observed in *Arabidopsis* mutants.**
402 The auxin sensitive analysis identified distinct and overlapping targets of ETT and ARF4. Targets under
403 the auxin-independent redundant regulation of ETT and ARF4 included the YABBY TFs *YAB2* and *YAB5*,
404 whilst *CRC* was mis-regulated in both *ett-3* and *ett-3 arf4*-2, consistent with its ETT-specific regulation.
405 YABBY proteins specify abaxial identity along with the KANADI family of transcription factors (Eshed
406 et al., 2004). ETT and ARF4 function co-operatively with KANADI proteins to promote abaxial cell fate
407 of lateral organs (Pekker et al., 2005). Laminal outgrowths from the abaxial leaf surface have
408 previously been observed in *kan1 kan2* loss of function mutants. This phenotype is suppressed in *yab1*
409 *yab3 yab5* (Eshed et al., 2004) and *yuc1 yuc2 yuc4* backgrounds (Wang et al., 2011), suggesting that
410 the production of outgrowths is dependent on YABBYs and auxin biosynthesis. Similar outgrowths
411 were observed on the abaxial surface of *ett arf4 arf2* triple mutants (Guan et al., 2017) and the *ett-3*
412 *arf4-2* mutant leaves in this study, consistent with previously proposed roles for ETT/ARF4 in KANADI-
413 mediated signalling (Pekker et al., 2005). However, given that *YAB2*, *YAB5,* and *CRC* were significantly
414 downregulated in the *ett-3 arf4-2* mutant background, it is unclear if these outgrowths are YABBY
415 dependent. Whilst *yabby* single mutants lack obvious abaxial-adaxial identity defects, higher order
416 mutants show significant alterations in abaxial-adaxial polarity (Sarojam et al., 2010; Siegfried et al.,
417 1999). The downregulation of multiple *YAB* transcription factors within the *ett-3 arf4-2* mutant is
418 therefore consistent with the abaxial-adaxial identity defects observed in the leaves and gynoecia of
419 the double mutant in this study.
420 Previous studies reported reduced valve margin definition in *ind* (Liljegren et al., 2004), and apical
421 gynoecium defects in *jag nub* and *crc* mutants (Dinneny et al., 2006; Bowman and Smyth, 1999).
422 Similar gynoecium defects were exhibited in this study by *ett-3* and *ett-3 arf4-2* (Fig. 1), along with the
423 constitutive downregulation of *IND, JAG,* and *CRC,* which is consistent with the previously proposed
424 roles of these genes in gynoecium development. Future studies should aim to determine which of the
425 targets identified within this study are direct/indirect ETT/ARF4 targets.
426

427 **Auxin Sensitive analysis suggests ETT and ARF4 maintain auxin insensitivity at target loci.**
428 Previous studies in *Marchantia polymorpha* and *Phiscomitrium patens* found antagonism between A-
429 and B-ARFs to regulate the auxin sensitivity of tissues (Kato et al., 2020; Lavy et al., 2016), with the
430 auxin response being promoted by A-ARFs and inhibited by B-ARFs. Consistent with this model of B-
431 ARF function, ETT and ARF4 were previously shown to repress auxin responses in an *Arabidopsis* root
432 hair system (Choi et al., 2018). The transcriptomics data presented here suggest that ETT and ARF4
433 largely prevent the auxin sensitivity of distinct and overlapping targets, many of which become
434 upregulated in response to auxin in various mutant backgrounds, consistent with models of A/B-ARF
435 antagonism.
436 However, many of their redundantly regulated targets, including genes involved in the regulation
437 of pectin become downregulated in response to auxin. Auxin-mediated repression has been observed
438 in TMK-mediated signalling, where atypical AUX/IAAs are stabilized in the presence of auxin (Cao et
439 al., 2019). However, it is unclear if such a mechanism functions in the gynoecium. Previous studies
440 have implicated PME family members in the regulation of cell wall stiffness during gynoecium
441 development in *ett* mutants and showed that ETT promotes PME expression in the carpels (Andres-
442 Robin et al., 2018; Andres-Robin et al., 2020). Furthermore, the overexpression of *PECTIN*
443 *METHYLESTERASE INHIBITOR 3* (*PMEI3*), which antagonises PME activity, phenocopied the valve
444 reductions observed in *ett* mutants (Andres-Robin et al., 2018). Taken together with these previous
445 studies, the data presented here suggest that ETT and ARF4 may redundantly promote the expression
446 of *PMEs* to prevent their downregulation in response to auxin, and the mis-regulation of these genes
447 may contribute to the gynoecium defects observed in *ett-3 arf4-2*.
448 The data presented suggest that ETT functions alongside ARF4 to prevent the expression of genes
449 which would otherwise become auxin sensitive in its absence, possibly through the activity of A-ARFs
450 with which they are co-expressed, or due to the activity of TMK-related pathways in the case of auxin-
451 downregulated genes. The data also suggest that the maintenance of genes in an auxin insensitive
452 state may be equally as important as the promotion of auxin sensitivity at other loci to facilitate normal
453 growth and development. This study demonstrates how dissecting the relationships between distinct
454 auxin signalling pathways is a powerful approach to gain a greater understanding of the wider auxin
455 signalling network, thereby broadening the perspective of auxin-mediated plant development.
456
457
458 **Materials and Methods**
459
460 **Plant materials and growth condition**

461 ***Arabidopsis*:** Seeds were sown onto damp soil (Levington F2 compost with Intercept and grit at a 6:1
462 ratio) and stratified for 3 days at 4°C in the dark before transferal to a controlled environment room
463 (CER) and growth in long day conditions (16 hours light/8 hours dark, 22°C). All mutant lines were
464 generated in a Col-0 background. Mutant and transgenic lines used in this work which have been
465 previously published are: *ett-3* (Sessions et al., 1997; Simonini et al., 2016), *arf4-2* (SALK_070506,
466 Alonso et al., 2003) and *tir1-1 afb2*-3 (Parry et al., 2009). The *ett-3 arf4-2* line was generated by
467 crossing the *ett-3* line and *arf4-2* (SALK_070506). The *tir1-1 afb2-3 ett-3* line was generated by crossing
468 *ett-3* with *tir1-1 afb2-3*. The PCR conditions and genotyping primers used for these lines are listed in
469 Table S4 and Table S5 respectively. *pARF3/ETT: GFP*, *pARF4: GFP*, *pARF5: GFP*, *pARF6: GFP* and *pARF8:*
470 *GFP* are previously published (Rademacher et al., 2011). The *pETT:GUS* line was previously published
471 in Kuhn et al., 2020.
472
473 ***Capsella*:** The genetic and expression analysis in *Capsella rubella* was conducted in the Cr22.5
474 background. The seeds were germinated on MS medium containing 10 µM Gibberellin at 22˚C. 10-
475 day-old seedlings were then transplanted to soil in 8cm pots and moved into a controlled environment
476 room (CER) at 22˚C, 16 hrs light and 20˚C 8 hrs dark conditions.
477
478 **Genotyping**
479 Genomic DNA was extracted from fresh young leaves by grinding with a micro- pestle in a 1.7 ml tube.
480 Arabidopsis extraction buffer was added (200 mM Tris HCl pH 7.7, 250 mM NaCl, 25 mM EDTA and
481 0.5% SDS) and the sample was ground for an additional 30 seconds. The sample was then centrifuged
482 at 15,000 x g in a table-top centrifuge for 5 minutes. The supernatant was transferred to a fresh 1.5
483 ml tube containing 200 µl isopropanol without disturbing the pellet. The sample was then inverted at
484 room temperature for 2 minutes. The sample then underwent centrifugation at 15,000 x g in a table-
485 top centrifuge for 7 minutes, and the supernatant was discarded. The pellet was then air dried for 20
486 minutes at room temperature and resuspended in 50 µl dH2O before being used as a template for
487 PCR or frozen at -20°C**.** SALK lines (*arf4-2 and afb2-3*) were genotyped in accordance with Alsonso et
488 al., 2003 using the primers and conditions specified in Table S4 and S5. Genotyping PCRs were
489 conducted using GoTaq DNA Polymerase (Promega) in accordance with the manufacturer's guidelines,
490 and with a final volume of 20 µl where genotype assessment occurred through gel electrophoresis
491 (*arf4-2 and afb2-3*), or 50 µl if genotype was to be assessed by sequencing (*ett-3*) or BsaI restriction
492 digestion (*tir1-1*). The *ett-3* EMS mutation causes a G to A substitution at position 2226 of the
493 *AT2G33860* genomic sequence. PCR was conducted using the primers specified in Table S4 and S5, to
494 amplify a 246bp product which was purified with a QIAquick PCR purification kit (Quiagen) before

495 sequencing. The *tir1-1* allele is an EMS mutation which introduces a G to A mutation in position 440
496 of the genomic *AT3G62980* sequence. A 517bp product was amplified using the primers specified in
497 Table S4 and S5 and digested with BsaI-HFv2 (NEB) according to the manufacturer's guidelines before
498 gel electrophoresis of the resulting product on 3% agarose gel. BsaI digestion of the PCR product in
499 the *tir1-1* mutant yields a single band of 517bp, whilst the wild type produces two bands of 437 and
500 80bp.
501
502 **Plasmid construction and plant transformation**
503 For the construction of the promoter: GUS reporter plasmids, the promoter regulatory sequences of
504 *CrAFB2* (1941bp), *CrAFB3* (2072bp), *CrTIR1* (2077bp), *CrARF4* (5324bp) and *CrETT* (3029bp), *AtAFB2*
505 (1086bp), *AtAFB2* (2049bp) and *AtTIR1* (2076bp) were isolated by PCR from genomic DNA and inserted
506 upstream of *GUS* gene of pCambia1301 vectors. For the construction of the CRISPR/Cas9 mediated
507 genome editing plasmids, DNA sequences encoding gRNAs adjacent to the PAM sequences (NGG)
508 were designed to target the first or second exons of gene of interest. The gRNAs were synthesised as
509 oligonucleotides with golden-gate cloning adapters and then were insert downstream of U6
510 promoters. The resulting gRNA plasmid were then recombined with *pRPS5a:Cas9z:E9t* and
511 hygromycin selection marker using golden-gate cloning methods to produce the binary vectors. All
512 vectors were verified by sequencing and introduced into *Agrobacterium tumefaciens* strain LBA4404
513 by electroporation.
514 Transformation of *Capsella* plants followed the methods described in Dong et al., 2022. The
515 transformants were screened on MS plants with 1% sucrose and 0.8% agar containing 40mg/L
516 hygromycin (Roche, no. 10843555001). For each construct, at least 10 independent transformants
517 were obtained for further analysis. For the CRISPR transformants, preliminary genotyping was
518 conducted using primers listed in the Table S6. Only the plants showing evidence of gene editing were
519 kept and processed into the T2 generation. For generating the Cas9-free homozygous mutant, the T2
520 CRISPR transformants were screened on MS plants with 1% sucrose and 0.8% agar containing 10mg/L
521 hygromycin. the hygromycin sensitive plants were isolated and genotyped again using primer listed in
522 Table S6. All the analysis were conducted on the T2 generation of the representative transgenic lines.
523 Additional information on the mutations induced in each line is available in Fig.S9.
524
525 **Auxin treatment, expression analysis and GUS staining**
526 For the auxin treatment, 100 µM IAA and 10 µM NPA working solutions were prepared with ethanol
527 and tween 20 (5%). The auxin and mock (water with 5% tween 20) solutions were dipped onto the
528 inflorescence after flowers from stage 13 onwards had been removed. The plants were then kept

529 under a vacuum for 5 mins and kept in humid condition in the CER under long-day condition
530 mentioned above for 1h.
531 The GUS histochemical assays were performed as previously described in Dong et al., 2019.
532 Specifically, inflorescence samples of *Capsella* or *Arabidopsis* were fixed in acetone for 20 mins at -
533 80°C, and then washed twice for 5 mins in 100 mM sodium phosphate buffer. The samples were then
534 processed in 100 mM sodium phosphate buffer containing 1mM $K_3Fe(CN)_6$, 1mM $K_4Fe(CN)_6$ at room
535 temperature for 30 mins to block the diffusion of GUS proteins. The staining process was conducted
536 at 37°C in the X-Gluc solution for 6-8h. The X-Gluc solution contains 100 mM sodium phosphate buffer,
537 10mM EDTA, 0.5 mM $K_3Fe(CN)_6$, 3 mM $K_4Fe(CN)_6$, 0.1% Triton X100 and 1 mg/ml of ß-glucoronidase
538 substrate X-gluc (5-bromo-4-chloro-3-indolyl glucuronide, MELFORD: B40020) dissolved in DMSO.
539 After staining, the reaction was suspended and replaced with 70% ethanol several times until
540 chlorophyll was completely washed out. Gynoecia or young fruits were dissected, mounted in
541 Chlorohydrate (Sigma number: 15307-500G-R) solution and analyzed using a Zeiss Axio Imager light
542 microscope.
543
544 **Scanning Electron Microscopy**
545 The Scanning Electron Microscopy (SEM) experiment followed the protocol in Dong et al., 2019.
546 Specifically, the gynoecia of each genotype were fixed in FAA and dissected. The samples were
547 critically-point dried in CO2 and sputter-coated with gold. The samples were subsequently examined
548 using a Zeiss Supra 55VP field Scanning Electron Microscope with an acceleration voltage of 3.0 kV.
549
550 **RNA sequencing Analysis (*Arabidopsis*)**
551 Whole inflorescences were harvested from Col-0, *ett-3*, *arf4-2,* and *ett-3 arf4-2* lines treated with
552 either mock (dH2O, 0.1% tween, 0.1% ethanol) or 100 µM IAA and 10µM NPA (dissolved in ethanol),
553 0.1% tween for one hour. Three biological replicates were harvested for each genotype one hour after
554 treatment. Each replicate contained pooled material from three plants. The tissue was snap frozen in
555 liquid nitrogen and RNA extraction was conducted using a Qiagen RNeasy Plant Mini Kit with on-
556 column DNase treatment, in accordance with the manufacturer's guidelines. The RNA quality was
557 assessed by gel electrophoresis, and the RNA concentration was measured using a nanodrop
558 (ThermoFisher), and the RNA integrity was tested using a Bioanalyzer 2100 (Agilent). Novogene (Hong
559 Kong), conducted cDNA library preparation (250-300 bp insert cDNA library), and sequencing (20M
560 pair reads). The mRNA was enriched using oligo-dT beads and fragmented before cDNA synthesis with
561 reverse transcriptase. First strand synthesis was conducted, and second strand synthesis buffer
562 (containing dNTPs, RNase H and E. coli polymerase I, Illumina) was added so that the second strand

563 was produced by nick- translation. The library was then purified and underwent terminal repair,
564 before A-tailing, ligation of sequencing adapters, size selection and PCR enrichment. Library
565 concentration was assessed using a Qubit 2.0 fluorometer (Life Technologies) and the strand sizes
566 were verified using a Bioanalyzer 2100 (Agilent) and qPCR. Raw Illumina sequencing data was then
567 converted to sequence reads using base calling. The error rate (0.03%) and A/T/G/C Content
568 Distribution were tested as a quality control, before data filtering to remove low quality reads, and
569 reads with adaptor contamination. Sequencing reads were mapped to the reference genome
570 (TAIR10), using HISAT2. Gene expression level was assessed using transcript abundance, which
571 assesses the number of Fragments Per Kilobase of transcript sequence per Millions base pairs
572 sequenced (FPKM). This method accounts for both the effects of sequencing depth and gene length
573 on fragment counting. HTSeq software was utilized in this analysis. Differentially Expressed Gene
574 (DEG) analyses utilized DESeq2 to conduct readcount normalization and negative binomial distribution
575 analysis ($p<0.05$) followed by the determination of the false discovery rate using the Benjamini and
576 Hochberg procedure ($p_{adjust}<0.05$). The FPKMs of all genes expressed in this analysis are available in
577 Supplemental data File 1.
578
579 **Principle Component Analysis**
580 Principle component analysis was conducted in iDEP 9.1 (http://ge- lab.org/idep/, (Ge et al., 2018) on
581 expression values normalised to fragments per kilobase of transcript per million mapped reads
582 (FPKM).
583
584 **Go Term Analysis**
585 Gene Ontology (GO) term analysis was conducted on the lists of genes which fell into each category
586 of the Venn diagrams in both the auxin independent and auxin sensitive analyses to identify whether
587 these lists were enriched for genes involved in specific biological processes. This GO term analysis was
588 conducted using shiny GO (version 0.77, Ge et al.,2020) using the default parameters (FDR cut off
589 =0.05). Gene lists were compared to all gene found to be expressed in the RNA seq analysis
590 (Supplemental data File 2)
591
592 **Analysis of auxin independent ETT/ARF4 targets**
593 This analysis was conducted using the differentially expressed gene lists provided by Novogene (Hong
594 Kong). Six lists of differentially expressed genes were used in this analysis: (1) *arf4-2* vs Col-0 mock; (2)
595 *ett-3* vs Col-0 mock; (3) *ett-3 arf4-2* vs Col-0 mock; (4) *arf4-2* vs Col-0 IAA; (5) *ett-3* vs Col-0 IAA; and
596 (6) *ett- 3 arf4-2* vs Col-0 IAA. Only genes which were at least 2-fold up or downregulated in at least

597 one background were included in this analysis (log2fold value of >1 or < -1). Analyses were conducted
598 with Venny (Version 2.1; https://bioinfogp.cnb.csic.es/tools/venny/index.html; Oliveros, 2007) to
599 identify genes mis-regulated only in one background, mis-regulated only in two backgrounds, or mis-
600 regulated in all three backgrounds relative to wild type. The mock and auxin treated datasets were
601 independently assessed using Venny, and then compared to identify genes which were similarly
602 differentially expressed in both the presence and absence of auxin. Finally, any genes which were
603 significantly differentially expressed (2-fold up or down-regulated in at least one background) in
604 response to auxin were removed from the lists, leaving only those genes which were regulated
605 independently of auxin. The output of this analysis is available in Supplemental data File 3.
606
607 **Analysis of auxin sensitive ETT/ARF4 targets**
608 The auxin sensitive analysis utilized DEGs from the following lists generated by Novogene (Hong Kong):
609 (1) Col-0 IAA vs Col-0 mock; (2) *ett-3* IAA vs *ett-3* mock; (3) *arf4-2* IAA vs *arf4-2* mock; and (4) *ett-3*
610 *arf4-2* IAA vs *ett-3 arf4-2* mock. The genes which were differentially expressed in each background in
611 response to auxin were then compared to reveal how the auxin response in each mutant differed from
612 WT. Venny (Version 2.1) was utilized to generate a four-way Venn diagram. The output of this analysis
613 is available in Supplemental data File 4.
614
615 **Yeast 2 Hybrid**
616 The full-length coding sequence of ETT and ARF4 and truncated ARF4 fragments were amplified by
617 PCR using primers designed for gateway cloning (Supplemental Table 6). The resulting PCR products
618 were purified using a Qiagen QIAquick PCR purification kit and introduced in the gateway entry vector
619 pDONR207 (Life Technologies) by BP clonase reactions, in accordance with the Thermo-Fisher
620 Gateway protocol. The products of this reaction were transformed into DH5α cells (Invitrogen)
621 according to the manufacturer's guidelines and grown on LB agar plates containing gentamycin (10
622 µg/ml) overnight at 37°C. Constructs were validated by colony PCR and sequencing. The ARF
623 sequences within pDONR207 were then recombined into the pGAD-T7 and pGBK-T7 (Clontech)
624 expression vectors by LR clonase reactions, transformed into E. coli, and once more validated by
625 colony PCR and sequencing. The expression vectors were then co-transformed into AH109
626 Saccharomyces cerevisiae (Clontech), by lithium acetate mediated transformation (Gietz and Schiestl,
627 2007). Different combinations of AD (pGAD-T7) and BD (pGBK-T7) vectors, or empty vector controls,
628 were introduced in pairs to competent yeast cells to determine whether ARF4 and ETT interact, and
629 through which domains of ARF4. Transformants were plated onto YSD -W-L media and grown at 28°C
630 for 72 hours, before serial dilution (10^0, 10^1, 10^2, and 10^3) and plated onto YSD -W-L-H-A plates to

assess interactions. After plating on selective media, yeast colonies were photographed after growth at 28°C for 7 days. Figures were created using images from the 10^1 dilution in all cases. Auxin sensitivity was assessed by adding 100 µM IAA (Sigma) to the medium.

Confocal Microscopy

Stage 8-14 gynoecia were dissected from the plant and placed onto slides in water containing 0.015% Silwet L-77 (De Sangosse Ltd.) to prevent the formation of bubbles. Cover slips were then applied, and the gynoecia were imaged using a Leica SP5 confocal microscope (HyD detector, Smart Gain 30% 200hz, 4x Line Average) with a 40x water immersion lens. GFP was excited at a wavelength of 488 nm and detected at 498–530 nm. Images were taken as Z-stacks, and then processed in Image J 1.48 to form composite 3D projections, which were then converted to RGB images.

Author contribution

H.M.M., Y.D. and L.Ø. devised the experiments. H.M.M. conducted the experiments in Arabidopsis with assistance from T. L. and B. N., Y.D. and T.L. conducted experiments in Capsella. H.M.M. wrote the manuscript. H.M.M., Y.D. and L.Ø revised the manuscript. All authors participated in the discussion of the data and in the production of the final version of the manuscript.

Acknowledgements

Apologies to any colleagues whose work we have not cited due to space limitations. Special thanks to Henrik Jönsson (SLCU) for supporting the completion of the project. Thanks to the JIC microscopy team and both JIC and SLCU horticulture teams for making this work possible. H.M.M. was funded by the John Innes Foundation (at JIC) and the Gatsby Charitable Foundation (at SLCU, GAT3395-PR4B), B.N. by BBSRC (BB/S002901/1) and L.Ø. by BBSRC (BB/P013511/1). The work in Capsella was supported by grants from the National Natural Science Foundation of China (32170227 and 32221001 to Y.D.) and K.C. Wong Education Foundation (GJTD-2020-05, received by Y.D.).

Competing interests: None to declare

References

Alonso, J. M., Stepanova, A. N., Leisse, T. J., Kim, C. J., Chen, H., Shinn, P., Stevenson, D. K., Zimmerman, J., Barajas, P., Cheuk, R., et al. (2003). Genome-wide insertional mutagenesis of Arabidopsis thaliana. *Science* **301**. doi: 10.1126/science.1086391.

Andres-Robin, A., Reymond, M. C., Dupire, A., Battu, V., Dubrulle, N., Mouille, G., Lefebvre, V., Pelloux, J., Boudaoud, A., Traas, J., et al. (2018). Evidence for the regulation of gynoecium morphogenesis by ETTIN via cell wall dynamics. *Plant Physiol* **178**. doi: 10.1104/pp.18.00745.

Andres-Robin, A., Reymond, M. C., Brunoud, G., Martin-Magniette, M. L., Monéger, F. and Scutt, C. P. (2020). Immediate targets of ETTIN suggest a key role for pectin methylesterase inhibitors in the control of Arabidopsis gynoecium development. *Plant Signal Behav* **15**. doi: 10.1080/15592324.2020.1771937.

Bowman, J. L. and Smyth, D. R. (1999). CRABS CLAW, a gene that regulates carpel and nectary development in Arabidopsis, encodes a novel protein with zinc finger and helix-loop-helix domains. *Development* **126**. doi: 10.1242/dev.126.11.2387.

Cao, M., Chen, R., Li, P., Yu, Y., Zheng, R., Ge, D., Zheng, W., Wang, X., Gu, Y., Gelová, Z., et al. (2019). TMK1-mediated auxin signalling regulates differential growth of the apical hook. *Nature* **568**. https://doi.org/10.1038/s41586-019-1069-7

Cecchetti, V., Altamura, M. M., Falasca, G., Costantino, P. and Cardarelli, M. (2008). Auxin regulates Arabidopsis anther dehiscence, pollen maturation, and filament elongation. *Plant Cell* **20**, 1760–1774. doi: 10.1105/tpc.107.057570.

Choi, H. S., Seo, M. and Cho, H. T. (2018). Two TPL-binding motifs of ARF2 are involved in repression of auxin responses. *Front Plant Sci* **9**. doi: 10.3389/fpls.2018.00372.

Davis, C. B., Johnston, S. B. and Ellis, J. P. (2020). Detecting and quantifying oligomerization of ARF PB1 Domains. *The FASEB Journal* **34**. https://doi.org/10.1096/fasebj.2020.34.s1.05777

Dharmasiri, N., Dharmasiri, S., Weijers, D., Lechner, E., Yamada, M., Hobbie, L., Ehrismann, J. S., Jürgens, G. and Estelle, M. (2005). Plant development is regulated by a family of auxin receptor F box proteins. *Dev Cell* **9**. doi: 10.1016/j.devcel.2005.05.014.

Dinneny, J. R., Weigel, D. and Yanofsky, M. F. (2006). NUBBIN and JAGGED define stamen and carpel shape in Arabidopsis. *Development* **133**. doi: 10.1242/dev.02335.

Dong, Y., Jantzen, F., Stacey, N., Łangowski, Ł., Moubayidin, L., Šimura, J., Ljung, K. and Østergaard, L. (2019). Regulatory Diversification of INDEHISCENT in the Capsella Genus Directs Variation in Fruit Morphology. *Current Biology* **29**. doi: 10.1016/j.cub.2019.01.057.

Dong, Y., Hu, Z. C. and Østergaard, L. (2022). An optimized protocol to assess SUMOylation in the plant Capsella rubella using two-component DEX-inducible transformants. *STAR Protoc* **3**. doi: 10.1016/j.xpro.2022.101197.

698 **Eshed, Y., Izhaki, A., Baum, S. F., Floyd, S. K. and Bowman, J. L.** (2004). Asymmetric leaf development
699 and blade expansion in Arabidopsis are mediated by KANADI and YABBY activities. *Development*
700 **131**. doi: 10.1242/dev.01186.
701 **Fendrych, M., Akhmanova, M., Merrin, J., Glanc, M., Hagihara, S., Takahashi, K., Uchida, N., Torii, K.**
702 **U. and Friml, J.** (2018). Rapid and reversible root growth inhibition by TIR1 auxin signalling. *Nat*
703 *Plants* **4**. doi: 10.1038/s41477-018-0190-1.
704 **Finet, C., Fourquin, C., Vinauger, M., Berne-Dedieu, A., Chambrier, P., Paindavoine, S. and Scutt, C.**
705 **P.** (2010). Parallel structural evolution of auxin response factors in the angiosperms. *Plant Journal*
706 **63**. doi: 10.1111/j.1365-313X.2010.04292.x.
707 **Finet, C., Berne-Dedieu, A., Scutt, C. P. and Marlétaz, F.** (2013). Evolution of the ARF gene family in
708 land plants: Old domains, new tricks. *Mol Biol Evol* **30**. doi: 10.1093/molbev/mss220.
709 **Friml, J., Gallei, M., Gelová, Z., Johnson, A., Mazur, E., Monzer, A., Rodriguez, L., Roosjen, M.,**
710 **Verstraeten, I., Živanović, B. D., et al.** (2022). ABP1–TMK auxin perception for global
711 phosphorylation and auxin canalization. *Nature* **609**, 575–581. doi: 10.1038/s41586-022-05187-
712 x.
713 **Ge, S. X., Son, E. W. and Yao, R.** (2018). iDEP: An integrated web application for differential expression
714 and pathway analysis of RNA-Seq data. *BMC Bioinformatics* **19**. doi: 10.1186/s12859-018-2486-
715 6.
716 **Ge, S. X., Jung, D., Jung, D. and Yao, R.** (2020). ShinyGO: A graphical gene-set enrichment tool for
717 animals and plants. *Bioinformatics* **36**. doi: 10.1093/bioinformatics/btz931.
718 **Gietz, R. D. and Schiestl, R. H.** (2007). High-efficiency yeast transformation using the LiAc/SS carrier
719 DNA/PEG method. *Nat Protoc* **2**. https://doi.org/10.1038/nprot.2007.13
720 **Guan, C., Wu, B., Yu, T., Wang, Q., Krogan, N. T., Liu, X. and Jiao, Y.** (2017). Spatial Auxin Signaling
721 Controls Leaf Flattening in Arabidopsis. *Current Biology* **27**. doi: 10.1016/j.cub.2017.08.042.
722 **Guilfoyle, T. J. and Hagen, G.** (2012). Getting a grasp on domain III/IV responsible for Auxin Response
723 Factor-IAA protein interactions. *Plant Science* **190**, 82–88. doi: 10.1016/j.plantsci.2012.04.003.
724 **Kato, H., Mutte, S. K., Suzuki, H., Crespo, I., Das, S., Radoeva, T., Fontana, M., Yoshitake, Y., Hainiwa,**
725 **E., van den Berg, W., et al.** (2020). Design principles of a minimal auxin response system. *Nat*
726 *Plants* **6**, 473–482. https://doi.org/10.1038/s41477-020-0662-y
727 **Kelley, D. R., Arreola, A., Gallagher, T. L. and Gasser, C. S.** (2012). ETTIN (ARF3) physically interacts
728 with KANADI proteins to form a functional complex essential for integument development and
729 polarity determination in Arabidopsis. *Development* **139**. doi: 10.1242/dev.067918.
730 **Kepinski, S. and Leyser, O.** (2005). The Arabidopsis F-box protein TIR1 is an auxin receptor. *Nature*
731 **435**. https://doi.org/10.1038/nature03542

Korasick, D. A., Chatterjee, S., Tonelli, M., Dashti, H., Lee, S. G., Westfall, C. S., Fulton, D. B., Andreotti, A. H., Amarasinghe, G. K., Strader, L. C., et al. (2015). Defining a two-pronged structural model for PB1 (Phox/Bem1p) domain interaction in plant auxin responses. *Journal of Biological Chemistry* **290**. doi: 10.1074/jbc.M115.648253.

Kuhn, A., Runciman, B., Tasker-Brown, W. and Østergaard, L. (2019). Two auxin response elements fine-tune pinoid expression during gynoecium development in arabidopsis thaliana. *Biomolecules* **9**. doi: 10.3390/biom9100526.

Kuhn, A., Harborough, S. R., McLaughlin, H. M., Natarajan, B., Verstraeten, I., Friml, J., Kepinski, S. and Østergaard, L. (2020). Direct ETTIN-auxin interaction controls chromatin states in gynoecium development. *Elife* **9**. doi: 10.7554/eLife.51787.

Łangowski, Ł., Stacey, N. and Østergaard, L. (2016). Diversification of fruit shape in the Brassicaceae family. *Plant Reprod* **29**. doi: 10.1007/s00497-016-0278-6.

Lavy, M., Prigge, M. J., Tao, S., Shain, S., Kuo, A., Kirchsteiger, K. and Estelle, M. (2016). Constitutive auxin response in Physcomitrella reveals complex interactions between Aux/IAA and ARF proteins. *Elife* ***5***. doi: 10.7554/eLife.13325.

Liljegren, S. J., Roeder, A. H. K., Kempin, S. A., Gremski, K., Østergaard, L., Guimil, S., Reyes, D. K. and Yanofsky, M. F. (2004). Control of fruit patterning in Arabidopsis by INDEHISCENT. *Cell* **116**. doi: 10.1016/s0092-8674(04)00217-x.

Moubayidin, L. and Østergaard, L. (2014). Dynamic control of auxin distribution imposes a bilateral-to-radial symmetry switch during gynoecium development. *Current Biology* **24**. doi: 10.1016/j.cub.2014.09.080.

Nagpal, P., Ellis, C. M., Weber, H., Ploense, S. E., Barkawi, L. S., Guilfoyle, T. J., Hagen, G., Alonso, J. M., Cohen, J. D., Farmer, E. E., et al. (2005). Auxin response factors ARF6 and ARF8 promote jasmonic acid production and flower maturation. *Development* **132**. doi: 10.1242/dev.01955.

Nemhauser, J. L., Feldman, L. J. and Zambryski, P. C. (2000). Auxin and ETTIN in Arabidopsis gynoecium morphogenesis. *Development* **127**. doi: 10.1242/dev.127.18.3877.

Oliveros, J. C. (2007). VENNY. An interactive tool for comparing lists with Venn Diagrams. http://bioinfogp.cnb.csic.es/tools/venny/index.html.*Bioinfogp.Cnb.Csic.Es/Tools/Venny/Index. Html*.

Paponov, I. A., Paponov, M., Teale, W., Menges, M., Chakrabortee, S., Murray, J. A. H. and Palme, K. (2008). Comprehensive transcriptome analysis of auxin responses in Arabidopsis. *Mol Plant* **1**, 321–337. doi: 10.1093/mp/ssm021.

764 **Parry, G., Calderon-Villalobos, L. I., Prigge, M., Peret, B., Dharmasiri, S., Itoh, H., Lechner, E., Gray,**
765 **W. M., Bennett, M. and Estelle, M.** (2009). *Complex regulation of the TIR1/AFB family of auxin*
766 *receptors*. *Proc Natl Acad Sci U S A* **106**. doi: 10.1073/pnas.0911967106.
767 **Pekker, I., Alvarez, J. P. and Eshed, Y.** (2005). Auxin response factors mediate Arabidopsis organ
768 asymmetry via modulation of KANADI activity. *Plant Cell* **17**. doi: 10.1105/tpc.105.034876.
769 **Piya, S., Shrestha, S. K., Binder, B., Neal Stewart, C. and Hewezi, T.** (2014). Protein-protein interaction
770 and gene co-expression maps of ARFs and Aux/IAAs in Arabidopsis. *Front Plant Sci* **5**, 1–9. doi:
771 10.3389/fpls.2014.00744.
772 **Prigge, M. J., Platre, M., Kadakia, N., Zhang, Y., Greenham, K., Szutu, W., Pandey, B. K., Bhosale, R.**
773 **A., Bennett, M. J., Busch, W., et al.** (2020). Genetic analysis of the arabidopsis TIR1/AFB auxin
774 receptors reveals both overlapping and specialized functions. *Elife* **9**. doi: 10.7554/eLife.54740.
775 **Rademacher, E. H., Möller, B., Lokerse, A. S., Llavata-Peris, C. I., Van Den Berg, W. and Weijers, D.**
776 (2011). A cellular expression map of the Arabidopsis AUXIN RESPONSE FACTOR gene family. *Plant*
777 *Journal* **68**. doi: 10.1111/j.1365-313X.2011.04710.x.
778 **Sarojam, R., Sappl, P. G., Goldshmidt, A., Efroni, I., Floyd, S. K., Eshed, Y. and Bowmana, J. L.** (2010).
779 Differentiating Arabidopsis shoots from leaves by combined YABBY activities. *Plant Cell* **22**. doi:
780 10.1105/tpc.110.075853.
781 **Sessions, R. A. and Zambryski, P. C.** (1995). Arabidopsis gynoecium structure in the wild type and in
782 ettin mutants. *Development* **121**. doi: 10.1242/dev.121.5.1519.
783 **Sessions, A., Nemhauser, J. L., McColl, A., Roe, J. L., Feldmann, K. A. and Zambryski, P. C.** (1997).
784 ETTIN patterns the Arabidopsis floral meristem and reproductive organs. *Development* **124**. doi:
785 10.1242/dev.124.22.4481.
786 **Siegfried, K. R., Eshed, Y., Baum, S. F., Otsuga, D., Drews, G. N. and Bowman, J. L.** (1999). Members
787 of the YABBY gene family specify abaxial cell fate in Arabidopsis. *Development* **126**. doi:
788 10.1242/dev.126.18.4117.
789 **Simonini, S., Deb, J., Moubayidin, L., Stephenson, P., Valluru, M., Freire-Rios, A., Sorefan, K., Weijers,**
790 **D., Friml, J. and Østergaard, L.** (2016). A noncanonical auxin-sensing mechanism is required for
791 organ morphogenesis in Arabidopsis. *Genes Dev* **30**. doi: 10.1101/gad.285361.116.
792 **Simonini, S., Bencivenga, S., Trick, M. and Østergaard, L.** (2017). Auxin-induced modulation of ETTIN
793 activity orchestrates gene expression in Arabidopsis. *Plant Cell* **29**. doi: 10.1105/tpc.17.00389.
794 **Simonini, S., Stephenson, P. and Østergaard, L.** (2018). A molecular framework controlling style
795 morphology in Brassicaceae. *Development* **145**. doi: 10.1242/dev.158105.
796 **Szemenyei, H., Hannon, M. and Long, J. A.** (2008). TOPLESS mediates auxin-dependent transcriptional
797 repression during Arabidopsis embryogenesis. *Science* **319**. doi: 10.1126/science.1151461.

Tiwari, S. B., Hagen, G. and Guilfoyle, T. (2003). The roles of auxin response factor domains in auxin-responsive transcription. *Plant Cell* **15**. doi: 10.1105/tpc.008417.

Ulmasov, T., Hagen, G. and Guilfoyle, T. J. (1999). Activation and repression of transcription by auxin-response factors. *Proc Natl Acad Sci U S A* **96**. doi: 10.1073/pnas.96.10.5844.

Vernoux, T., Brunoud, G., Farcot, E., Morin, V., van den Daele, H., Legrand, J., Oliva, M., Das, P., Larrieu, A., Wells, D., et al. (2011). The auxin signalling network translates dynamic input into robust patterning at the shoot apex. *Mol Syst Biol* **7**. doi: 10.1038/msb.2011.39.

Wang, J. W., Wang, L. J., Mao, Y. B., Cai, W. J., Xue, H. W. and Chen, X. Y. (2005). Control of root cap formation by MicroRNA-targeted auxin response factors in Arabidopsis. *Plant Cell* **17**, 2204–2216. doi: 10.1105/tpc.105.033076.

Wang, W., Xu, B., Wang, H., Li, J., Huang, H. and Xu, L. (2011). YUCCA genes are expressed in response to leaf adaxial-abaxial juxtaposition and are required for leaf margin development. *Plant Physiol* **157**. doi: 10.1104/pp.111.186395.

Figures:

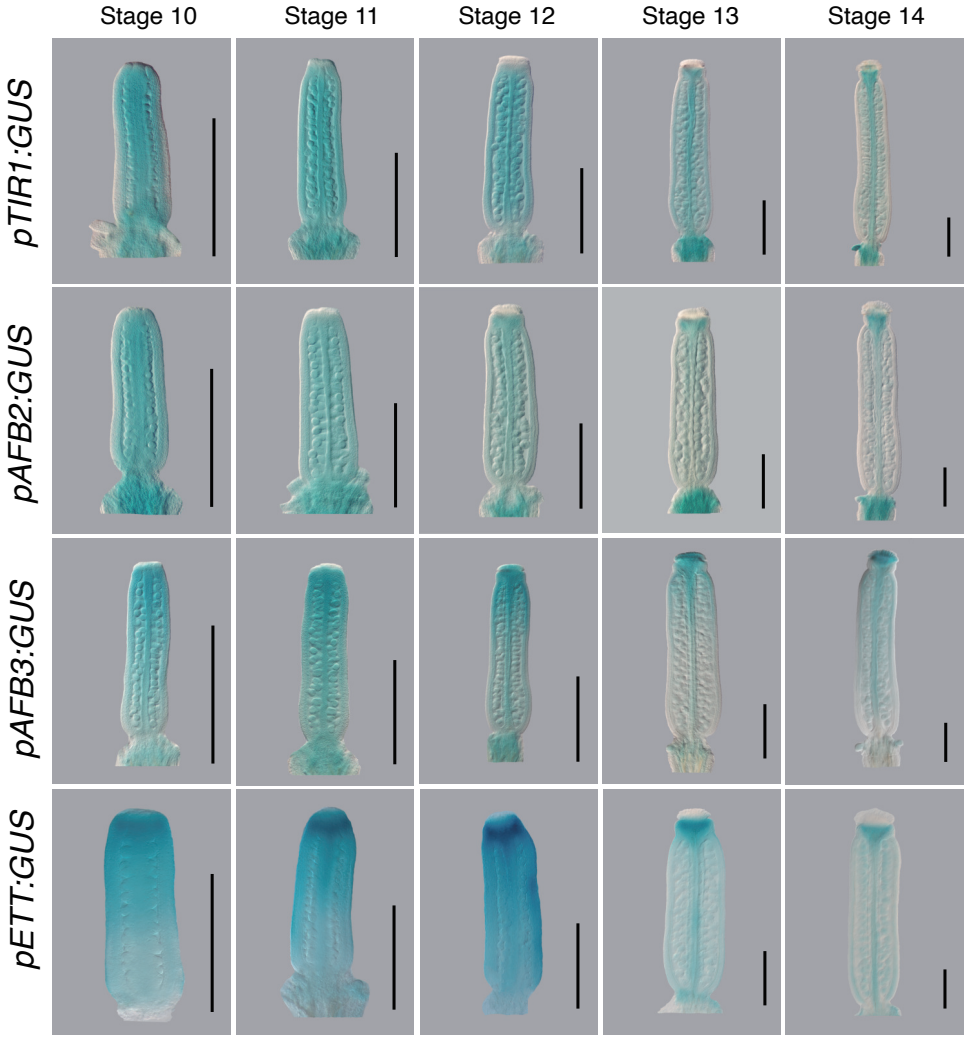

Fig. 1: Expression analysis of genes involved in the canonical and ETT-mediated auxin signalling pathway in *Arabidopsis thaliana.* GUS staining showing the expression patterns of *pAtETT, pAtTIR1*, *pAtAFB2* and *pAtAFB3* from stage 10-14 of gynoecium development. Scale bars 500μm.

849

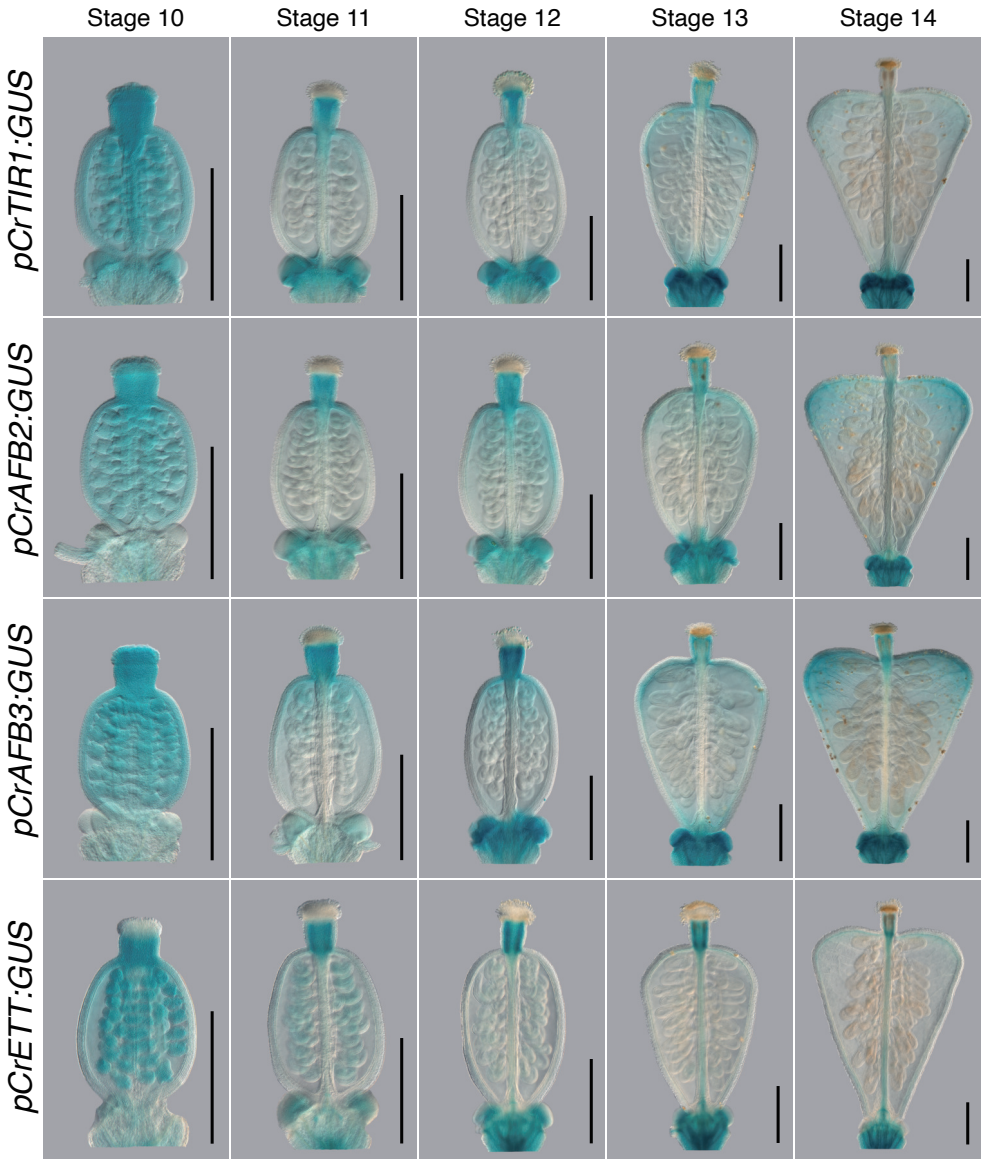

850

851 **Fig. 2: Expression analysis of genes involved in the canonical and ETT-**
852 **mediated auxin signalling pathway in *Capsella rubella*.** GUS staining showing the
853 expression patterns of *pCrETT, pCrTIR1*, *pCrAFB2* and *pCrAFB3* from stage 10-14 of
854 gynoecium development. Scale bars 500μm.

855

856

857

858

859

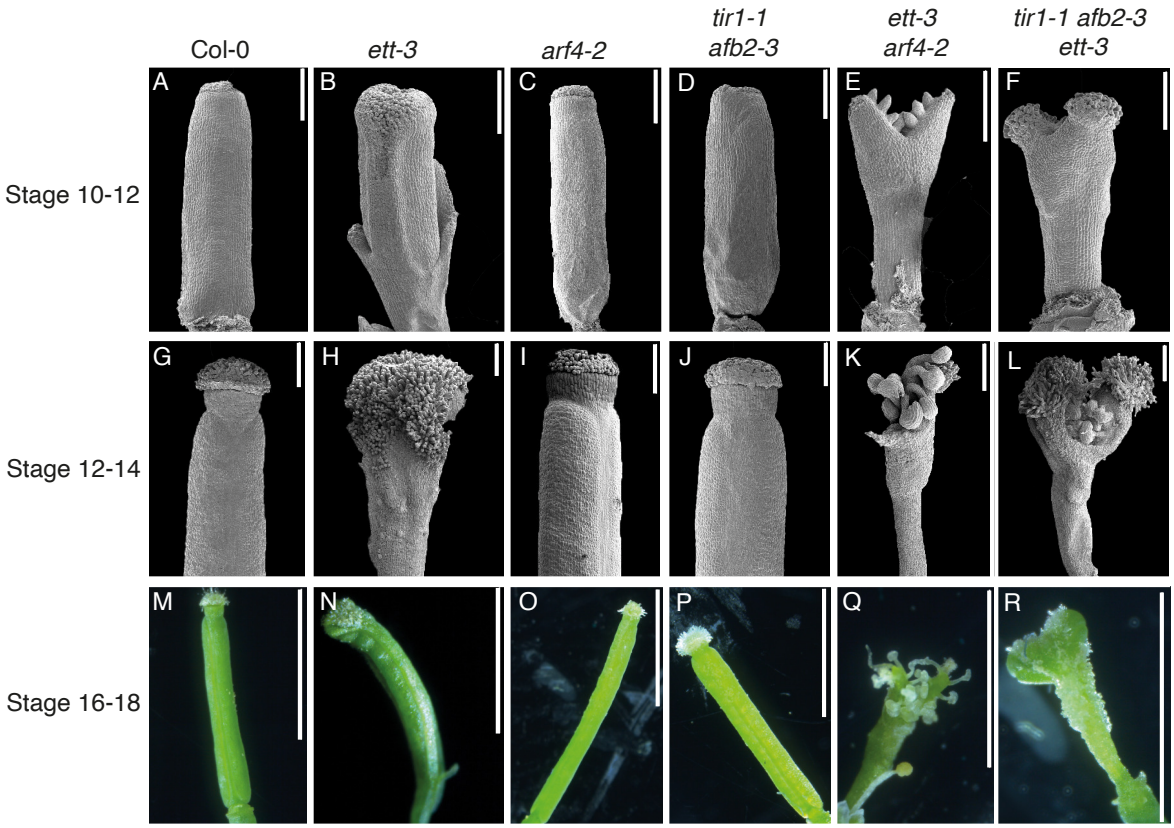

Fig. 3: Phenotypic analysis of *Arabidopsis* gynoecium defects in canonical and ETT-mediated pathway mutants reveals synergism in gynoecium development. Scanning electron micrographs (stage 10-12, stage 12-14), and photographs (stage 16-18) of gynoecia from WT (A, G, M), *ett-3* (B, H, N), *arf4-2* (C, I, O), *tir1-1 afb2-3* (D, J, P), *ett-3 arf4-2* (E, K, Q), and *tir1-1 afb2-3 ett-3* (F, L, R) mutants in *Arabidopsis*. Scale bars in SEM 200μm, Scale bars in photographs 3cm

877

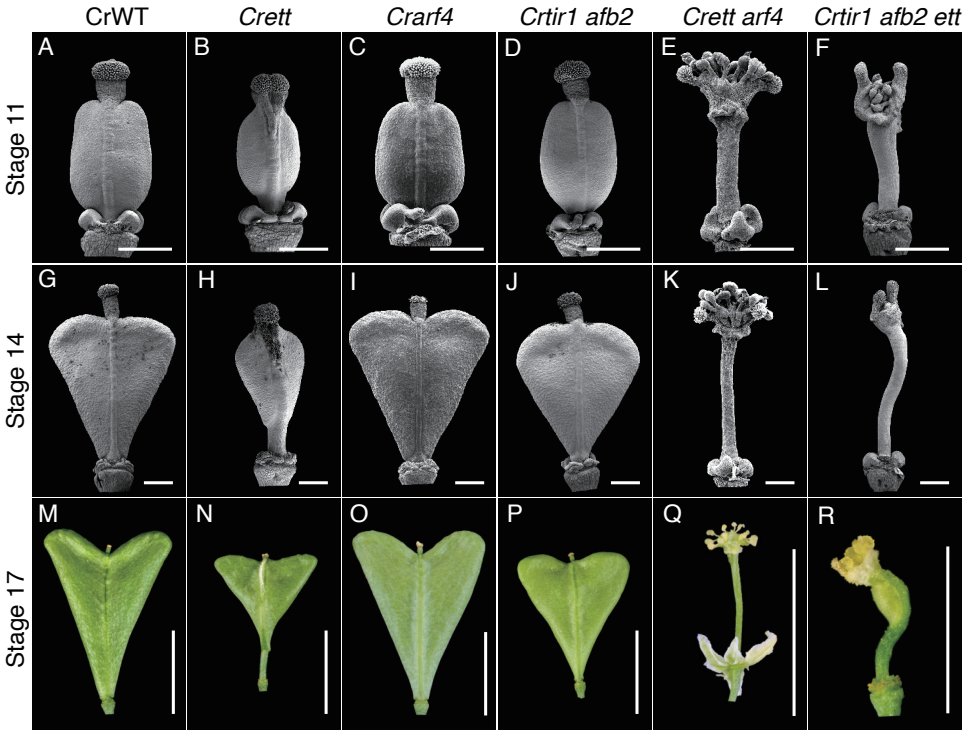

878

879 **Fig. 4: Phenotypic analysis of *Capsella* gynoecium defects in canonical and**
880 **ETT-mediated pathway mutants reveals conserved synergism in gynoecium**
881 **development.** Scanning electron micrographs (stage 11, stage 14), and photographs
882 (stage 17) of gynoecia from WT (A, G, M), *ett* (B, H, N), *arf4* (C, I, O), *tir1 afb2* (D, J,
883 P), *ett arf4* (E, K, Q), and *tir1 afb2 ett-* (F, L, R) mutants in *Capsella,* Scale bars in
884 SEM 200 μm, Scale bars in photographs 0.5 cm

885

886

887

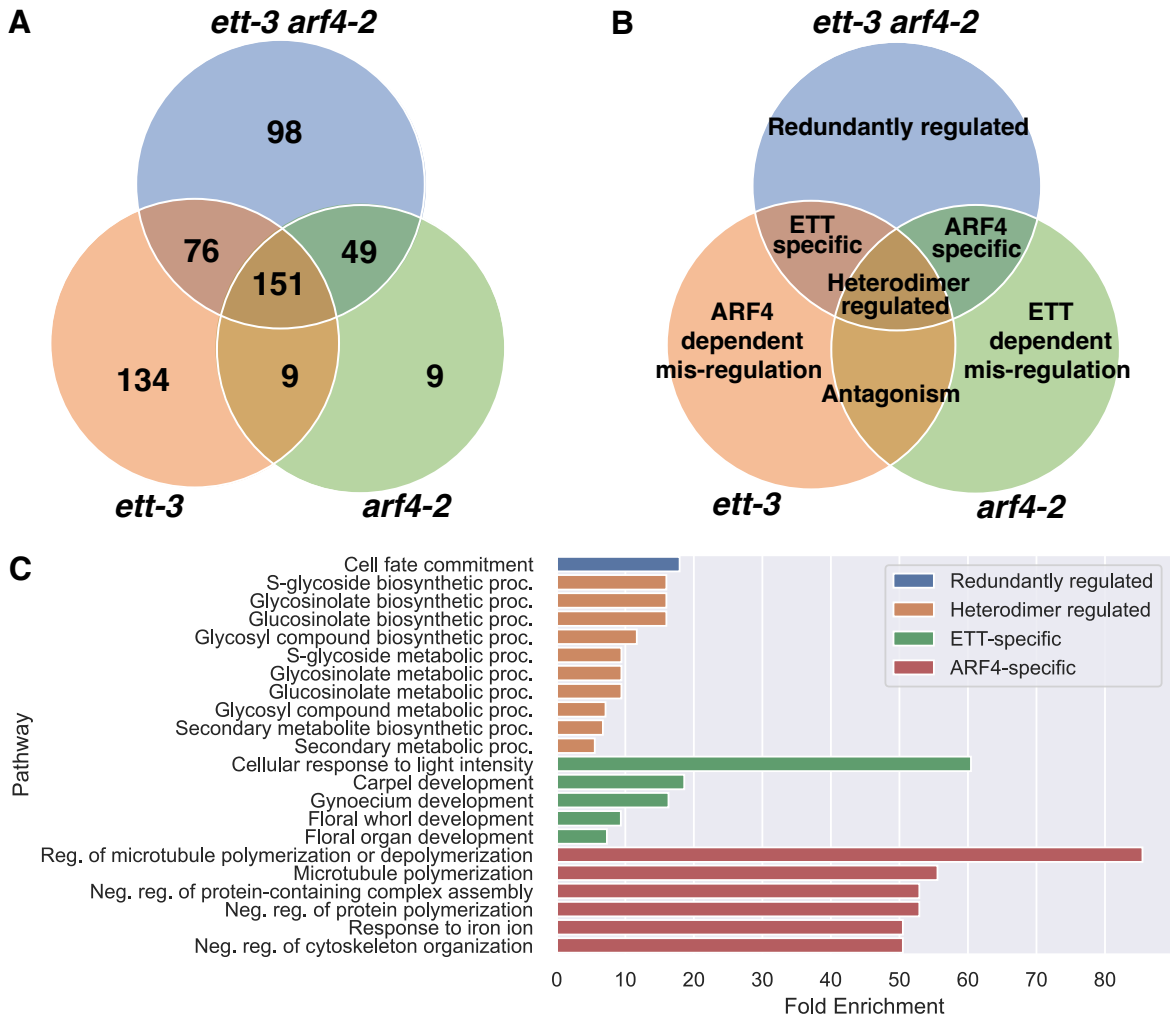

Fig. 5: Summary of genes identified in comparative-RNA seq experiments as ETT/ARF4 targets regulated independently of auxin. A) The numbers of genes falling within each segment of a three way venn diagram comparing genes which are significantly differentially independently of auxin in ett-3, arf4-2 and ett-3 arf4-2 mutants compared to wildtype. B) Summary of the relationship between ETT/ARF4 and the genes within each Venn diagram segment. C) Significant GO terms identified for lists of genes in each Venn diagram segment.

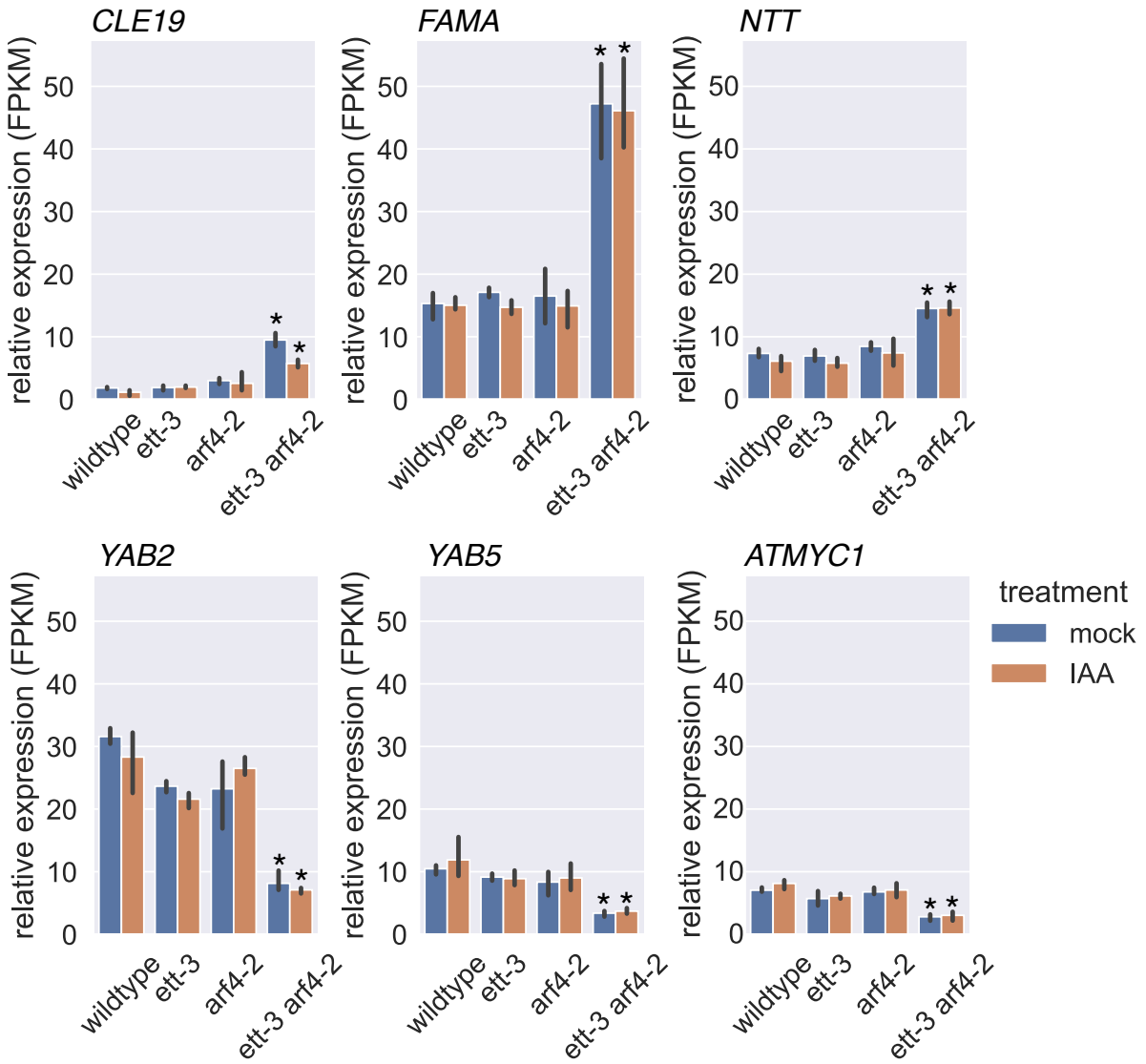

Fig. 6: The normalized expression of genes which are redundantly regulated by ETT and ARF4 independently of auxin, and which were identified in GO term analysis as genes involved in the regulation of cell fate commitment. *CLE19, CLAVATA3/ESR-RELATED 19, NTT, NO TRANSMITTING TRACT, YAB2, YABBY2, YAB5, YABBY5, ATMYC1, ARABIDOPSIS THALIANA MYC1.* FPMK, fragments per kilobase per million mapped fragments. Statistical analysis was conducted using read count normalization, negative binomial distribution analysis and FDR correction using the BH procedure. The error bars show +/- standard deviation * = Padjust<0.05 vs the same treatment in wildtype.

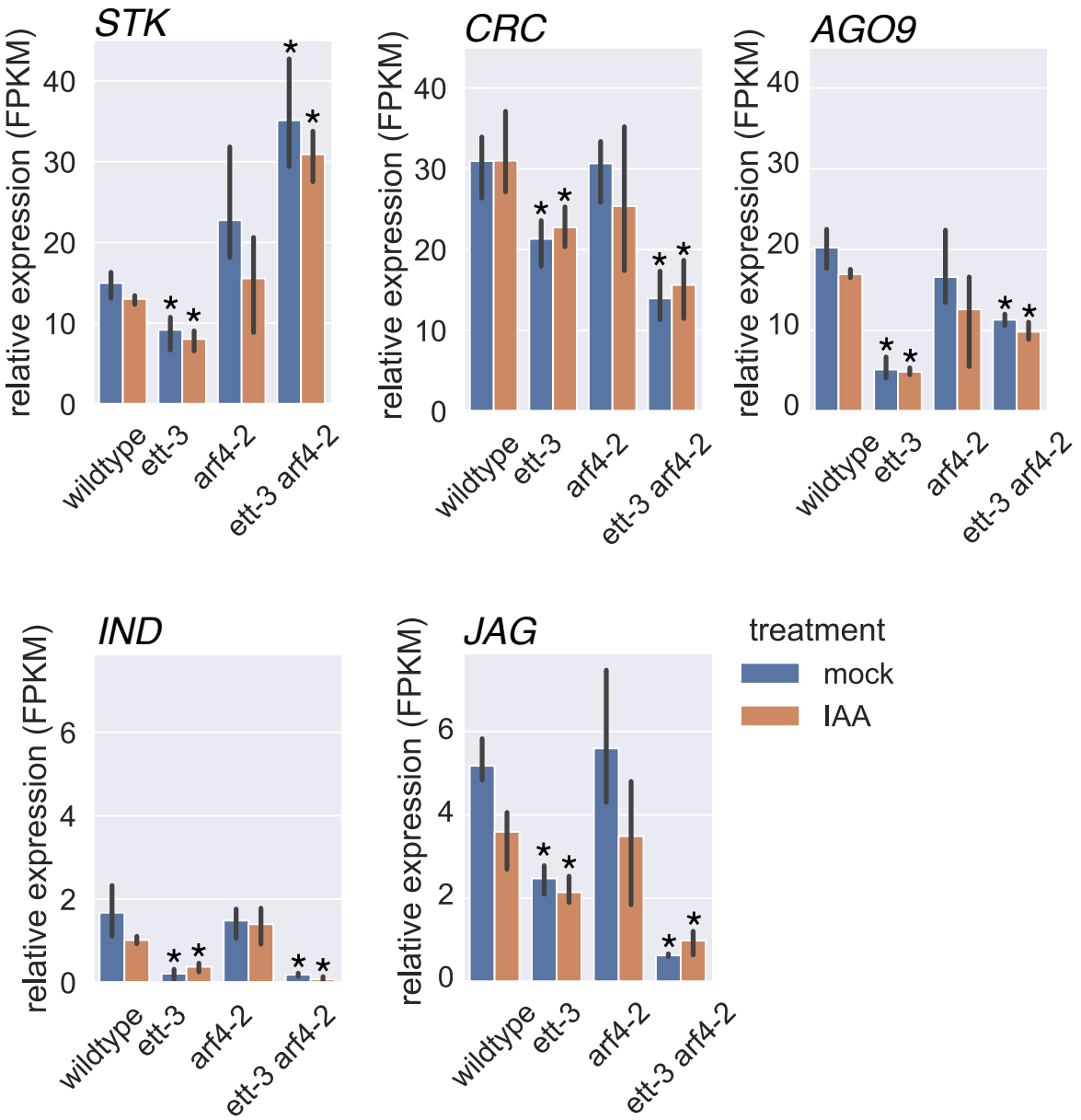

Fig. 7: The normalized expression of genes identified in GO term analysis as involved in gynoecium development which are differentially expressed in *ett-3* and *ett-3 arf4-2* relative to wildtype, consistent with their ETT-specific regulation. *STK*, *SEEDSTICK*, *CRC*, *CRABSCLAW*, *AGO9*, *ARGONAUT9*, *IND*, *INDEHISCENT*, *JAG*, *JAGGED*. FPMK, fragments per kilobase per million mapped fragments. Statistical analysis was conducted using read count normalization, negative binomial distribution analysis and FDR correction using the BH procedure. The error bars show +/- standard deviation * = Padjust<0.05 vs the same treatment in wildtype.

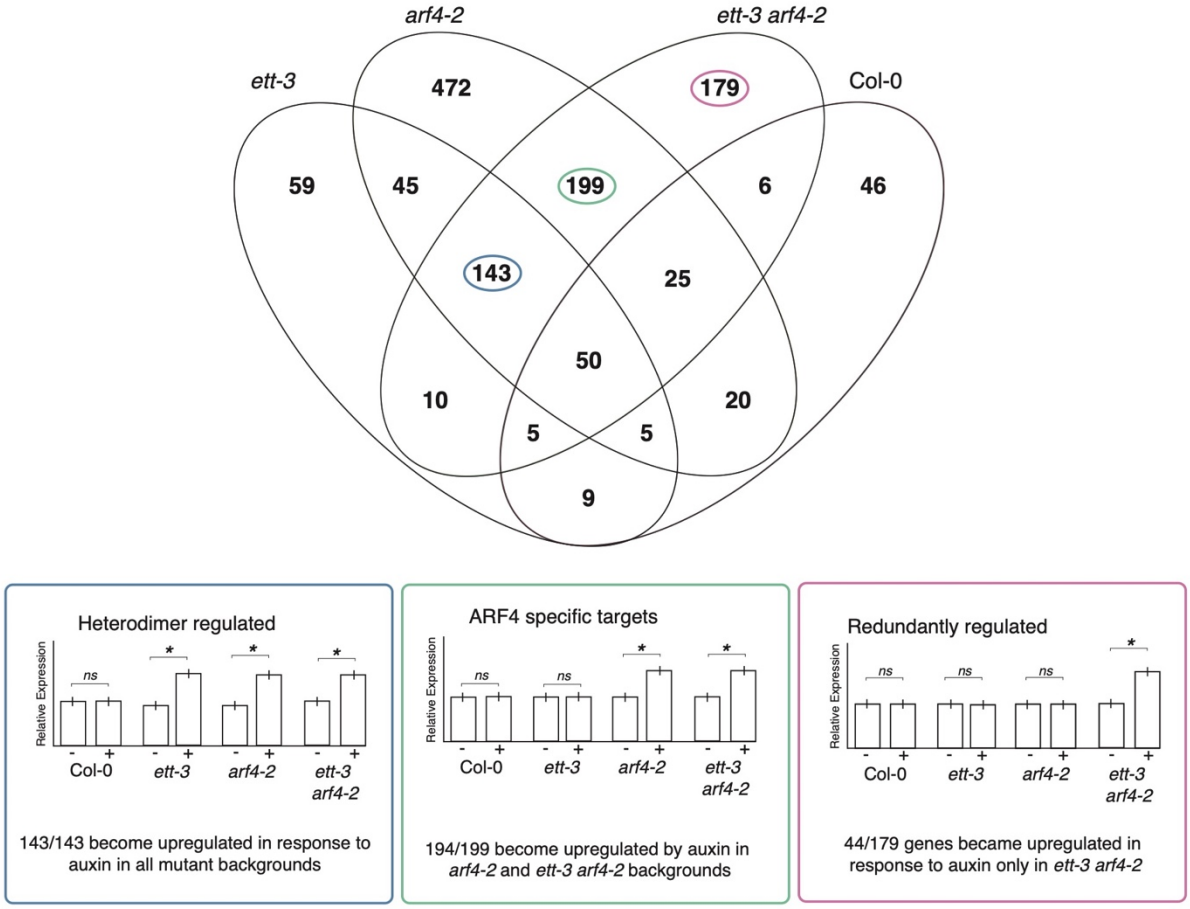

Fig. 8: Summary of the outcome of the auxin sensitive comparative RNA-sequencing analysis comparing the auxin response in ett-3, arf4-2, or ett-3 arf4-2 to the auxin response in wildtype. Groups of genes which conform to models of A-B ARF antagonism, and their expression profiles are highlighted below.

944

945

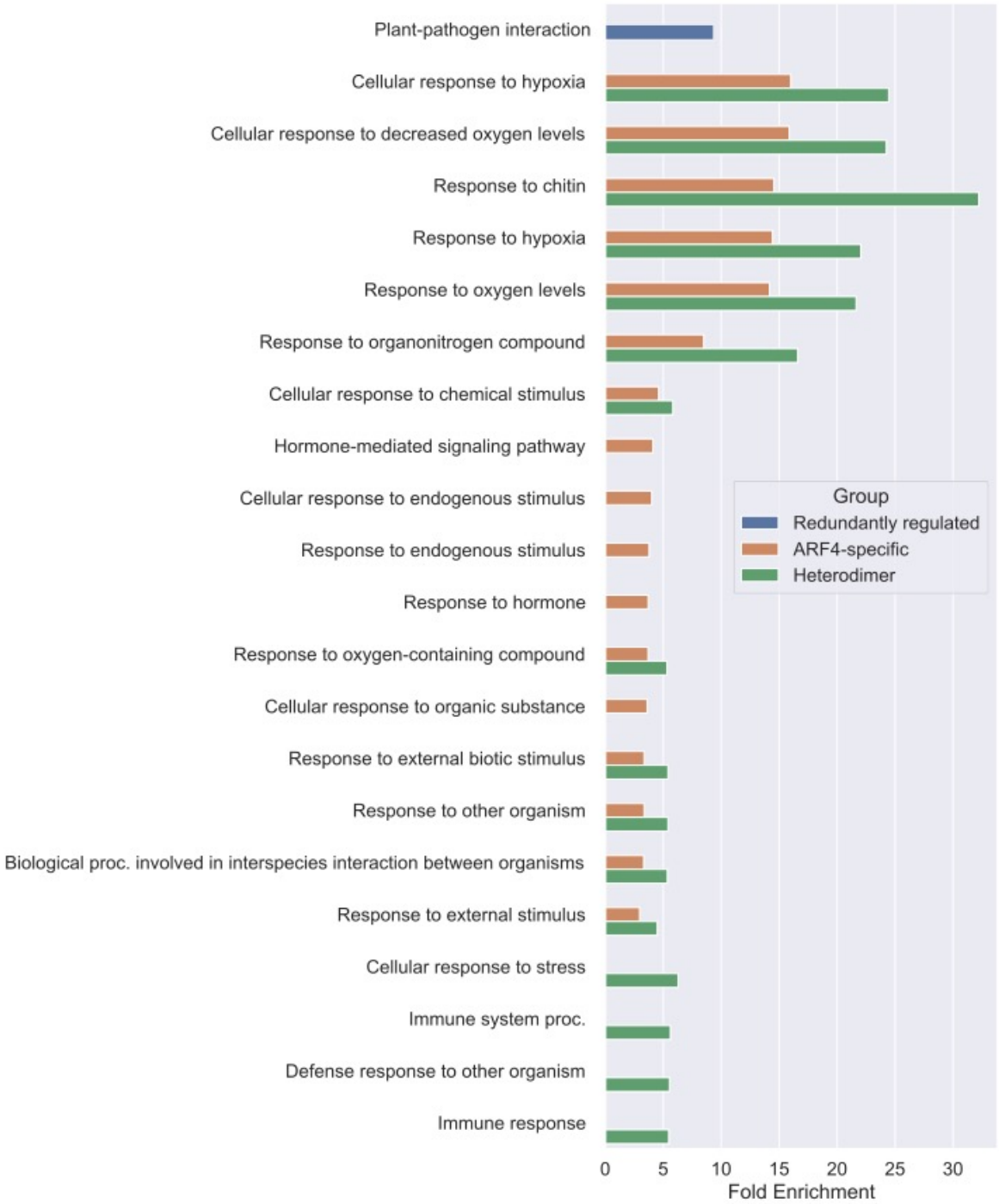

946

947 **Fig. 9: GO terms which are significantly enriched in lists of genes which conform**

948 **to models of A-B ARF antagonism.**

949